frontiers in Marine Science

ORIGINAL RESEARCH
published: 12 January 2022
doi: 10.3389/fmars.2021.759603

Toward a Solution of the "Peruvian Puzzle": Pelagic Food-Web Structure and Trophic Interactions in the Northern Humboldt Current Upwelling System Off Peru

Jana C. Massing[1,2,3], Anna Schukat[1], Holger Auel[1], Dominik Auch[4], Leila Kittu[5], Elda Luz Pinedo Arteaga[6], Jonathan Correa Acosta[6] and Wilhelm Hagen[1]*

[1] BreMarE – Bremen Marine Ecology, Marine Zoology, Universität Bremen (FB 02), Bremen, Germany, [2] Helmholtz Institute for Functional Marine Biodiversity at the University of Oldenburg (HIFMB), Oldenburg, Germany, [3] University of Bremen and Alfred Wegener Institute, Helmholtz Centre for Polar and Marine Research, Bremerhaven, Germany, [4] IMF – Institute of Marine Ecosystem and Fishery Science, University of Hamburg, Hamburg, Germany, [5] GEOMAR Helmholtz Centre for Ocean Research Kiel, Kiel, Germany, [6] Instituto del Mar del Perú (IMARPE), Callao, Peru

OPEN ACCESS

Edited by:
Chiara Piroddi,
Joint Research Centre, Italy

Reviewed by:
Ruben Escribano,
University of Concepción, Chile
Leonardo Castro,
University of Concepción, Chile

****Correspondence:***
Jana C. Massing
jana.massing@hifmb.de

Specialty section:
This article was submitted to Marine Ecosystem Ecology, a section of the journal Frontiers in Marine Science

Received: *16 August 2021*
Accepted: *20 December 2021*
Published: *12 January 2022*

Citation:
Massing JC, Schukat A, Auel H, Auch D, Kittu L, Pinedo Arteaga EL, Correa Acosta J and Hagen W (2022) Toward a Solution of the "Peruvian Puzzle": Pelagic Food-Web Structure and Trophic Interactions in the Northern Humboldt Current Upwelling System Off Peru. Front. Mar. Sci. 8:759603. doi: 10.3389/fmars.2021.759603

The northern Humboldt Current upwelling system (HCS) belongs to the most productive marine ecosystems, providing five to eight times higher fisheries landings per unit area than other coastal upwelling systems. To solve this "Peruvian puzzle", to elucidate the pelagic food-web structure and to better understand trophic interactions in the HCS, a combined stable isotope and fatty acid trophic biomarker approach was adopted for key zooplankton taxa and higher trophic positions with an extensive spatial coverage from 8.5 to 16°S and a vertical range down to 1,000 m depth. A pronounced regional shift by up to ∼5‰ in the δ^{15}N baseline of the food web occurred from North to South. Besides regional shifts, δ^{15}N ratios of particulate organic matter (POM) also tended to increase with depth, with differences of up to 3.8‰ between surface waters and the oxygen minimum zone. In consequence, suspension-feeding zooplankton permanently residing at depth had up to ∼6‰ higher δ^{15}N signals than surface-living species or diel vertical migrants. The comprehensive data set covered over 20 zooplankton taxa and indicated that three crustacean species usually are key in the zooplankton community, i.e., the copepods *Calanus chilensis* at the surface and *Eucalanus inermis* in the pronounced OMZ and the krill *Euphausia mucronata*, resulting in an overall low number of major trophic pathways toward anchovies. In addition, the semi-pelagic squat lobster *Pleuroncodes monodon* appears to play a key role in the benthic-pelagic coupling, as indicated by highest δ^{13}C' ratios of −14.7‰. If feeding on benthic resources and by diel vertical migration, they provide a unique pathway for returning carbon and energy from the seafloor to the epipelagic layer, increasing the food supply for pelagic fish. Overall, these mechanisms result in a very efficient food chain, channeling energy toward higher trophic positions and partially explaining the "Peruvian puzzle" of enormous fish production in the HCS.

Keywords: zooplankton, trophic position, biomarker, fatty acids, stable isotopes

INTRODUCTION

The northern Humboldt Current upwelling system (HCS) off Peru in the Pacific Ocean holds the world's largest single-species fishery with a fish production per unit area that is higher than in any other region of the world ocean (Bertrand et al., 2004; Chavez et al., 2008; Castillo et al., 2019). The Peruvian anchovy fishery on *Engraulis ringens* alone provided up to ∼10% of the global marine fish catch in certain years. While ranked only third in primary production in comparison to the other three Eastern Boundary Upwelling Systems (EBUS), i.e., the Benguela, California, and Canary Current systems, the HCS provides a 5–10 times higher fishery yield (Carr, 2002; Chavez et al., 2008). This apparent paradox, the "Peruvian Puzzle", though already targeted in various studies (e.g., Bakun and Weeks, 2008; Chavez and Messié, 2009; Espinoza et al., 2017), is not yet fully understood. It is clear that the trophic positions and interactions in between primary producers and commercially harvested fish, i.e., different zooplankton taxa, must play a critical role in the efficient transfer of energy along the food web, sustaining the outstanding fish production in the northern HCS. The present study focuses on the specific roles of key zooplankton taxa in the pelagic food web to elucidate the mechanisms that explain such a high trophic transfer efficiency (TTE) in the HCS and, thus, the enormous fish production.

Zooplankton species, especially copepods and euphausiids, are essential food sources for anchovies and sardines in the HCS, and thus important components of the food web. Acting as a crucial link, but also as an energy consumer between primary production and higher trophic positions (Ayón et al., 2008b), zooplankton plays a key role in terms of TTE. In coastal upwelling regions, copepods comprise up to 90% of the mesozooplankton in terms of abundance (Loick et al., 2005; Verheye et al., 2005). Their roles are very diverse and complex (e.g., Schukat et al., 2014), and details about their trophic positions, interactions and feeding behavior are needed in order to understand the functioning of the ecosystem.

Stable isotopes and fatty acids as trophic biomarkers provide integrated dietary information and allow to assess trophic positions and dietary preferences (Minagawa and Wada, 1984; Graeve et al., 1994; Dalsgaard et al., 2003). Stable isotope ratios of carbon ($\delta^{13}C$) and nitrogen ($\delta^{15}N$) elucidate the basic carbon source and trophic positions, respectively (e.g., Minagawa and Wada, 1984). Heavier isotopes accumulate in the body tissues of consumers, whereas lighter ones are preferably metabolized and excreted owing to fractionation during food assimilation (France and Peters, 1997). The enrichment in $\delta^{15}N$ by 3–4‰ per trophic position can be used to determine the trophic positions of consumers relative to their diets or preys (Minagawa and Wada, 1984). In contrast, carbon transported through the food web shows little change in the $\delta^{13}C$ signature (0.4–1.0‰ per trophic position). Therefore, the $\delta^{13}C$ ratio can be used to identify different sources of carbon and primary production at the basis of the food web (e.g., Post, 2002). The fatty acid trophic marker (FATM) concept is based on the findings that consumers incorporate typical fatty acids of certain phyto- and zooplankton groups without modification, which enables us to follow them through the food web (Kattner et al., 1994; Dalsgaard et al., 2003). The two biomarker approaches complement each other: Stable isotope ratios provide trophic positions, while fatty acid analyses reveal dietary preferences and predator-prey relationships.

Hitherto, zooplankton trophic positions and interactions in the HCS have not been well established, despite their importance in the ecosystem. Previous studies pooled zooplankton, copepods and/or euphausiids, as one group occupying the same trophic position or treated them as one "black" box within a certain range of trophic positions (e.g., Jarre-Teichmann, 1998; Espinoza et al., 2017). Such a simplistic view with a low taxonomic resolution does not reflect the complex diversity of zooplankton taxa and provides little insights into their role in the energy transfer.

The aim of this study is to "open" the zooplankton "black box" and to better understand the trophic interactions and the pelagic food-web structure in the HCS. Therefore, a large data set of key zooplankton taxa and higher trophic positions with an extensive spatial coverage was analyzed, and trophic interactions were evaluated using the combined biomarker approach of fatty acids and stable isotopes. Specifically, we test the following four hypotheses:

(i) The northern HCS off Peru is characterized by a regional shift in the $\delta^{15}N$ baseline of the food web from North to South hampering direct regional comparisons of $\delta^{15}N$-derived trophic positions. In order to cope with this methodological challenge, here we apply an alternative approach of defining a $\delta^{15}N$ food-web reference based on salps as herbivorous consumers.

(ii) Besides regional shifts in the $\delta^{15}N$ signal, there are also vertical differences in $\delta^{15}N$ ratios and, hence, calculated trophic positions of zooplankton species from different depth layers. The $\delta^{15}N$ ratio of POM increases with depth. In consequence, the $\delta^{15}N$ signals of suspension-feeding zooplankton permanently residing at depth are higher than those of surface-living species or diel vertical migrants feeding at night in the surface layer.

(iii) Since only relatively few biomass-rich crustacean species dominate the HCS zooplankton community, the overall food-web structure is rather simple with only a restricted number of major trophic pathways relevant for channeling most of the energy from primary production to anchovies. Such a highly efficient food web may partly solve the "Peruvian Puzzle" of enormous pelagic fish stocks and landings despite primary production rates similar to other EBUS.

(iv) Finally, the endemic squat lobster *Pleuroncodes monodon* plays a key role in the benthic-pelagic coupling in the HCS. By partly feeding on benthic resources and performing diel vertical migrations, the species provides a unique pathway for returning carbon and energy from the seafloor to the epipelagic layer, where it becomes available as prey for pelagic fishes. This re-import of organic matter into the euphotic zone may also contribute to the exceptionally high trophic transfer efficiency of the HCS.

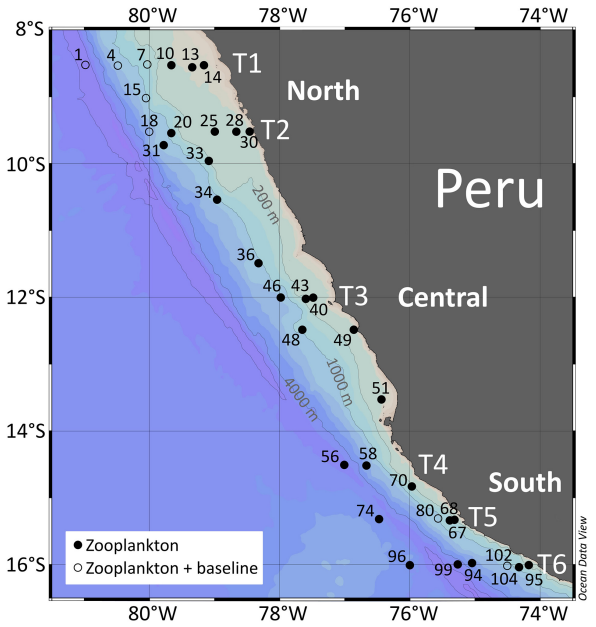

FIGURE 1 | Sampling stations in the Humboldt Current upwelling system off Peru providing zooplankton (solid circles) and zooplankton together with baseline samples (open circles). The sampled area was divided into northern (stns. 1–34), central (stns. 36–51), and southern regions (stns. 56–104) as indicated by the different transects (T1–T6).

MATERIALS AND METHODS

Sampling

As part of the CUSCO project (Coastal Upwelling System in a Changing Ocean), zooplankton and nekton organisms were sampled during the research cruise MSM 80 on board RV *Maria S. Merian* in the Humboldt Current upwelling system off Peru between 8°30′S and 17°00′S in December 2018/January 2019 (**Figure 1**). Due to low to moderate wind velocities, upwelling intensity was rather moderate during the entire cruise with sea surface temperatures between 17 and 24°C, usually around 22°C.

Different plankton nets were deployed to collect the organisms: a multiple opening/closing net system (Hydro-Bios Multinet) and an Isaacs-Kidd Midwater Trawl (IKMT: 10 m^2, mesh size 4 mm). Most of the organisms were collected by stratified vertical hauls with a Multinet Midi: mouth opening 0.25 m^2, mesh size 200 µm, five nets (for station plan see **Figure 1**). At shallow stations close to the coast, the entire water column was sampled, whereas in deeper waters, maximum sampling depth was 1,000 m (for details of sampling stations see **Supplementary Appendix Table 1**). Immediately after each haul, specimens were sorted alive in the lab (for smaller organisms a dissecting microscope was used for identification). Apparently live and healthy individuals were stored in vials and deep-frozen at −80°C until further lipid and stable isotope analyses in Germany. At one station dinoflagellate samples were collected by bucket sampling in a red tide, i.e., red-brown-colored surface water. Bits of feathers were gathered from seabirds that landed on board during the night and were released the next morning. Fish was sampled opportunistically. We collected some fish in the IKMT and some were caught incidentally on a drifter mooring. For surface particulate organic matter (POM)/bulk seston samples, water (250–2,000 mL) was collected from CTD casts (for sampling details see **Supplementary Appendix Table 2**) and filtered under gentle pressure (200 mbar) through pre-combusted GF/F filters (Whatman, 25 mm Ø, 0.3 µm nominal pore size). Filters were acidified with 2 mL of 1 M HCl for 2 min to remove any inorganic carbon. The filters were transferred to 2 mL cryovials and stored at −20°C until further analysis at GEOMAR in Kiel, Germany. The majority of samples was frozen at −80°C and transported home by air freight on dry ice. Some samples were transferred into tin capsules and dried onboard for stable isotope analysis in Germany. If possible, samples for lipid and stable isotope analyses were taken from the same stations, net and depth intervals.

Lipid and Fatty Acid Analysis

Total Lipid Extraction

Prior to lipid analysis, deep-frozen specimens were lyophilized for 48 h and their dry mass (DM) was determined gravimetrically. To obtain sufficient biomass for the analysis (>1 mg DM) smaller zooplankton specimens of the same species and stage were pooled from the same station and sampling depth. For fishes, muscle tissue from the rear end was used for the analysis. Total lipid was extracted with dichloromethane/methanol (DCM/MeOH, 2:1 per volume) (Hagen et al., 2000). A Potter homogenizer as well as an ultrasonic cell disrupter were used for homogenization of the samples. Aqueous KCl solution (0.88%) was added prior to centrifugation and phase separation (Folch et al., 1957). The extracted total lipid mass (TL) was determined gravimetrically and expressed as % of dry mass (%DM).

Transmethylation and Fatty Acid Analysis

Transesterification induced by hexane and methanol with 3% concentrated sulfuric acid converted fatty acids to their methyl ester derivatives (Kattner et al., 1994). Using a gas chromatograph (Agilent Technologies 7890A) equipped with a DB-FFAP column of 30 m length and 0.25 mm inner diameter and a programmable temperature vaporizer injector, fatty acids (FAs) and fatty alcohols (FAlcs) were simultaneously separated and quantified.

FAs and FAlcs were identified by comparing their retention times with those of known standards. Unknown FA and FAlc components with less than 1% contribution to total fatty acids or alcohols in all samples were excluded from further analysis. Mass spectrometry data were kindly provided by Dr. Graeve (AWI) to identify unknown peaks with a significant area. The amounts of wax esters were calculated from the FAlc levels, assuming that the FAlc comprised 50% of the mass of the wax ester molecules (Kattner et al., 2003).

Evaluation

Following the trophic biomarker concept, FA compositions were evaluated: The FAs 16:0, 20:5(n–3) and 22:6(n–3) are typical components of biomembranes (e.g., Dalsgaard et al., 2003). The latter polyunsaturated fatty acids EPA and DHA were not used

as fatty acid trophic markers (FATM), since these fatty acids are dominant components of biomembranes (phospholipids), but dietary information *via* FATM is incorporated in storage lipids like triacylglycerols and wax esters. Therefore, the relative contents of EPA and DHA increase much more during starvation than during feeding on diatoms or dinoflagellates, respectively, as biomembrane lipids gain dominance when storage lipids decline. High levels of 16:1(*n*–7) as well as 16:4(*n*–1) and 18:1(*n*–7) indicate a diatom-dominated diet, 18:4(*n*–) is a marker FA for dinoflagellates (e.g., Dalsgaard et al., 2003). Typical FAs synthesized by calanid copepods are 20:1(*n*–9) and 22:1(*n*–11) (Kattner and Hagen, 1995). The FA 18:1(*n*–9) is used as a carnivory marker (e.g., Dalsgaard et al., 2003). To assess the proportion of carnivorous compared to herbivorous feeding, the following modified carnivory index was applied (Bode et al., 2015):

$$CI = 18{:}1(n{-}9)/[16{:}1(n{-}7) + 16{:}4(n{-}1) + 18{:}1(n{-}7) + 18{:}4(n{-}3) + 18{:}1(n{-}9)]$$

GraphPad PRISM (version 5.01; GraphPad Software, La Jolla, CA, United States[1]) and PRIMER (version 6.1.6; Plymouth Marine Laboratory, Prospect Place, Plymouth PL1 3DH, United Kingdom) were used to conduct all statistical analyses. The Kolmogorov–Smirnov test, D'Agostino and Pearson omnibus normality test and Shapiro–Wilk normality test were used, if data were normally distributed. The *t*-test for data with a Gaussian distribution or the Mann–Whitney test for distribution-free data were used to test for species- or group-specific differences. For overall comparisons of groups, one-way ANOVA and *post hoc* test (Tukey) or Kruskal–Wallis and Dunn's test were used for normally distributed and distribution-free data, respectively. *P*-values < 0.05 indicate a significant difference.

To compare FA compositions with regard to taxon-specific and/or region- and depth-related differences, a Principal Component Analysis (PCA) was conducted. Variability in FAlc composition was not considered to avoid a separation of species depending on wax-ester storage. We considered all marker FAs and FAs with mean values >3% (group percentage). Prior to PCA, the FA percentages were arcsine-square-root transformed to ensure normality and homogeneity of variance.

Stable Isotope Analysis

For the determination of stable isotopes ($\delta^{13}C$ and $\delta^{15}N$), approximately 1 mg of freeze dried (lyophilized) sample of the same species and stage was transferred into a tin capsule and weighed using a microbalance (Sartorius, NCII1S, precision ± 10 μg). To provide sufficient biomass for the isotope analysis, smaller specimens of the same species and almost always the same stage were pooled. Most copepods were used completely, whereas for larger animals only parts were analyzed. Sections of feathers (non-destructive method) and parts of the caudal fin were used to determine stable isotope ratios of seabirds and fish, respectively. Using a mass spectrometer (EA NA1500 Series 2, Carlo Erba Instruments) and helium as carrier gas, stable isotope analyses were performed by Agroisolab GmbH in Jülich, Germany. Stable isotope ratios of carbon and nitrogen were determined using the IAEA-VPDB (IAEA-C1) and atmospheric air (IAEA-N1) as standards, respectively. Isotopic ratios are expressed as $\delta^{13}C$ and $\delta^{15}N$ in ‰, according to the equation given in Hobson et al. (2002). To avoid any bias of $\delta^{15}N$, lipids were not extracted before the isotope analysis (Hobson et al., 2002; Mintenbeck et al., 2008). As total lipid levels were highly variable among the organisms, $\delta^{13}C$ values were corrected considering the molar *C*/*N* ratios and employing a model, which normalizes ratios to a constant lipid content and is suitable for *C*:*N* ratios ≥ 4.0 (e.g., Smyntek et al., 2007; Mintenbeck et al., 2008). Lipid-corrected values are presented as $\delta^{13}C'$.

Particulate organic matter filter samples were oven dried at 60°C for 12 h and pelletized in tin capsules before being analyzed for POC/N concentration and isotopic composition ($\delta^{13}C/\delta^{15}N$). Isotopic composition was determined at GEOMAR using an elemental analyzer (Flash IRMS, Thermo Fisher) connected to a mass spectrometer (Delta V Advantage Isotope Ratio MS, Thermo Fisher) with the ConFlo IV interface (Thermo Fisher).

Determination of $\delta^{13}C$ and $\delta^{15}N$ From Preserved Net Samples

To maximize the number of samples and replicates for the regional comparison of species' isotopic composition of $\delta^{15}N$ (**Figure 2**), additional samples for stable isotope analysis were taken from preserved (4% formaldehyde in seawater solution) net samples (e.g., Bicknell et al., 2011). A correction factor (CF) for the formaldehyde-preserved samples was calculated by comparing the isotopic composition of preserved samples with that of deep-frozen (−80°C) samples from the same station and depth. For that purpose, preserved individuals were dried at 60°C and 1–2 mg of dry mass were transferred into tin capsules and sent to Agroisolab GmbH in Jülich, Germany, for measurements of $\delta^{13}C$ and $\delta^{15}N$. CFs for stable isotope ratios of $\delta^{13}C$ and $\delta^{15}N$ as well as for carbon (C) and nitrogen (N) content (in %) were determined based on formaldehyde-preserved (n = 35) and frozen samples (n = 42) (**Table 1**). In general, $\delta^{15}N$ increased by 1.2 ± 0.2‰ and $\delta^{13}C$ decreased by 1.0 ± 0.6‰ due to preservation.

Calculation of Trophic Position

We used two different approaches to determine a $\delta^{15}N$ baseline for the HCS food web:

i) POM samples (on filters) representing trophic position (TP) 1.
ii) Filter-feeding salps (*Iasis cylindrica*) as primary consumers representing TP 2.

Trophic positions were calculated *via* the equation:

$$TP = \lambda + (\delta^{15}N_{consumer} - \delta^{15}N_{reference})/\Delta_n$$

where λ is the TP of the organism used to estimate $\delta^{15}N_{reference}$ and Δ_n is the enrichment in $\delta^{15}N$ per TP. We applied the common average enrichment of 3.4‰ per TP (Peterson and Fry, 1987; Hobson and Welch, 1992).

[1]www.graphpad.com

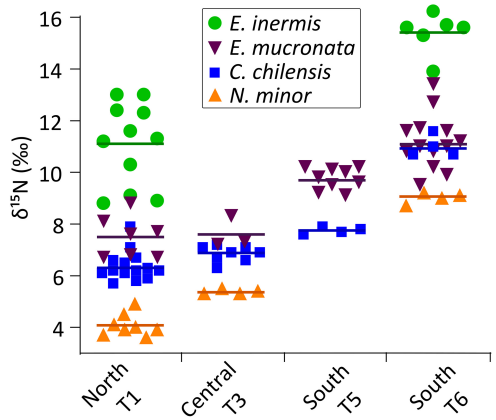

FIGURE 2 | Regional differences in $\delta^{15}N$ isotope ratios of key crustacean species of the northern HCS off Peru. Copepod species *Calanus chilensis* and *Nannocalanus minor*, the OMZ-inhabiting *Eucalanus inermis* and the vertically migrating key krill species *Euphausia mucronata* from the northern transect (T1) via the central transect (T3) to the southern transects (T5 and T6). Lines indicate medians. All samples for one species were collected from the same depth layers.

RESULTS

Hydrography

Upwelling intensity was low to moderate during the entire sampling period according to low wind velocities and sea surface temperatures usually ranging between 22 and 24°C on the northern and 20 and 22°C on the southern Peruvian shelf. The upper 10 m of the water column were generally well ventilated with oxygen levels >150 μmol L^{-1}. On the shelf, the oxygen minimum zone (OMZ, <45 μmol L^{-1}) usually extended from 30 m depth to the seafloor with almost anoxic conditions (<1 μmol L^{-1}) above the seafloor. Along the northern offshore transects, the OMZ spanned from ∼60 to ∼950 m depth with an anoxic core between 200 and 500 m. At the central and southern offshore stations, the OMZ was shallower, ranging from ∼30/40 m down to ∼900–1,000 m depth or the seafloor. Anoxic conditions occurred from ∼100 or 150–450 m.

Zooplankton Dry Mass and Total Lipid Content

Copepod DM ranged between 0.06 ± 0.01 mg DM $ind.^{-1}$ in female *Centropages brachiatus* and 0.54 ± 0.03 mg DM $ind.^{-1}$ in female *Euchaeta rimana*. Among the euphausiids, *Nematoscelis* sp. represented the smallest species with 4.9 ± 0.9 mg DM $ind.^{-1}$ and 15–17 mm body length, whereas *Euphausia eximia* (13.3 ± 5.9 mg DM $ind.^{-1}$, body length: 16–25 mm) represented the heaviest euphausiid in this study. The most abundant euphausiid *Euphausia mucronata* reached a similar mean dry mass of 12.1 ± 5.2 mg DM $ind.^{-1}$ and a body length of 20.2 ± 2.3 mm. Among the decapods, *Gennadas* sp. comprised the smallest specimens with 88.2 ± 16.3 mg DM $ind.^{-1}$ (body length: 22–35 mm), while adult squat lobsters *P. monodon* weighed on average 234.1 ± 47.3 mg DM $ind.^{-1}$ (body length: 30–40 mm). The heaviest decapod was *Acanthephyra* sp. with 665 ± 319.0 mg DM $ind.^{-1}$ and body lengths of 48–70 mm (**Table 2**).

Total lipid (TL) levels were usually moderate, with lowest values of 2.0 ± 0.1% DM in salps and highest in the deeper-living peracarid *Gnathophausia* sp. (47.8 ± 2.1% DM). Copepod lipid levels ranged from 7.5 ± 1.4% DM in *Subeucalanus mucronatus* to 16.3 ± 5.7% DM in copepodite stage C5 of *Calanus chilensis*. In comparison to the C5 copepodids, *C. chilensis* females exhibited slightly lower lipid levels of 13.4 ± 4.2% DM. Lipid contents of

TABLE 1 | Correction factors (CFs) to compensate for changes in stable isotope ratios, carbon, and nitrogen content of copepod samples caused by formaldehyde-preservation (C5: copepodid 5; f: females).

Copepod species	Stage	Cruise	Station	Depth (m)	*n*	$\delta^{13}C$	$\delta^{15}N$	%C	%N
Metridia lucens	f	M100-1	1874	180–20	3	1.03	1.14	1.51	1.37
Metridia lucens	f	M100-1	1876	20–0	3	1.08	1.22	1.64	1.29
Calanoides natalis	f	M100-1	1874	80–20	3	1.00	1.38	1.08	0.96
Calanus chilensis	f	MSM 80	4	50–0	3–4	1.03	1.21	1.97	2.02
Calanus chilensis	C5	MSM 80	4	50–0	3–4	1.06	1.14	1.49	1.33
Nannocalanus minor	f	MSM 80	7	20–0	3	1.07	1.35	1.50	1.45
Euchaeta rimana	f	MSM 80	7	20–0	8	1.06	1.22	1.38	1.48
Mean CF						1.05 ± 0.03	1.24 ± 0.09	1.51 ± 0.25	1.41 ± 0.29
Water-rich copepod									
Eucalanus inermis	f	MSM 80	1	600–400	3–4	1.02	0.73	2.66	2.21
Eucalanus inermis	f	MSM 80	4	500–200	4	1.06	0.66	2.35	1.68
Eucalanus inermis	f	MSM 80	94	50–0	2–5	1.03	0.81	1.90	1.56
Mean CF						1.04 ± 0.02	0.73 ± 0.06	2.30 ± 0.31	1.81 ± 0.28

Measurement results of formaldehyde-preserved samples have to be multiplied with the respective CF to provide realistic values for unpreserved conditions. Besides data from the HCS based on samples from the research cruise MSM 80, table also includes data from the Benguela Current upwelling system derived from research cruise M100-1 and analyzed accordingly with the same methods. n: number of analyses.

TABLE 2 | Dry mass (DM), total lipid (TL), wax ester (WE) contents, fatty acid (FA) and fatty alcohol (FAlc) compositions of zooplankton and fishes of the northern HCS.

	Gastropoda	Calanoid copepoda										Cyclopoid Cop.
	Pterotrachea sp.	*C. chilensis*			*N. minor*	*E. inermis*		*S. mucronatus*	*E. rimana*	*C. brachiatus*	*Acartia* sp.	Bulk
		C5	m	f	f	C5	f	C5	f	f	f	
n (ind)	3	8 (219)	3 (90)	16 (451)	3 (80)	2 (18)	3 (12)	3 (90)	3 (30)	5 (130)	1	3
Dry mass (mg ind^{-1})	192.32 ± 39.56	0.16 ± 0.02	0.17 ± 0.01	0.24 ± 0.03	0.09 ± 0.01	0.19/0.21	0.44 ± 0.01	0.11 ± 0.03	0.54 ± 0.03	0.06 ± 0.01	N.A.	N.A.
Total lipid (% DM)	1.4 ± 0.5	16.3 ± 5.7	12.7 ± 0.9	13.4 ± 4.2	N.A.	39.9/11.1	14.5 ± 5.5	7.5 ± 1.4	10.8 ± 3.0	12.8 ± 6.0	12.3	8.9 ± 0.4
Wax esters (% TL)	–	57.4 ± 15.5	65.0 ± 2.7	38.8 ± 11.7	–	–	–	–	29.4 ± 0.7	–	–	41.1 ± 1.2
Fatty acids (% TFA)												
14:0	1.8 ± 0.4	5.9 ± 2.1	7.2 ± 0.4	4.9 ± 1.5	3.6 ± 0.4	2.6/4.0	3.0 ± 1.7	6.7 ± 1.3	1.6 ± 0.2	2.9 ± 0.6	5.0	7.2 ± 0.6
16:0	11.3 ± 3.2	12.4 ± 1.7	11.7 ± 0.3	13.1 ± 1.7	12.8 ± 0.1	19.1/19.6	17.2 ± 1.8	16.2 ± 0.1	12.8 ± 0.3	14.0 ± 0.8	13.4	13.0 ± 0.5
16:1(*n*–7)	0.9 ± 0.4	5.0 ± 2.4	6.0 ± 0.7	6.7 ± 1.9	1.4 ± 0.1	3.7/5.4	6.9 ± 4.1	5.9 ± 0.5	2.0 ± 0.1	3.4 ± 0.4	4.1	8.0 ± 0.7
16:4(*n*–1)	–	1.0 ± 0.6	–	1.0 ± 0.5	–	0.0/0.4	0.4 ± 0.2	2.3 ± 0.2	–	0.8 ± 0.3	0.9	1.4 ± 0.1
18:0	5.8 ± 0.2	2.8 ± 1.0	3.7 ± 0.2	3.0 ± 0.6	4.5 ± 0.2	4.0/5.2	2.6 ± 0.2	2.6 ± 0.2	2.5 ± 0.2	3.1 ± 0.4	2.7	2.5 ± 0.1
18:1(*n*–7)	1.4 ± 0.2	0.7 ± 0.0	0.5 ± 0.0	0.7 ± 0.1	0.7 ± 0.0	2.1/2.2	3.8 ± 0.5	2.7 ± 0.1	0.8 ± 0.0	2.0 ± 0.0	1.1	0.9 ± 0.0
18:1(*n*–9)	4.5 ± 1.4	3.2 ± 1.0	3.1 ± 0.3	3.0 ± 0.8	2.2 ± 0.1	7.3/8.8	5.4 ± 0.5	4.4 ± 0.2	11.2 ± 0.4	1.2 ± 0.2	1.1	4.3 ± 0.5
18:2(*n*–6)	2.2 ± 0.4	1.3 ± 0.2	1.5 ± 0.3	1.3 ± 0.5	1.2 ± 0.0	1.6/1.7	1.3 ± 0.2	2.5 ± 0.0	1.3 ± 0.0	0.9 ± 0.0	0.9	1.5 ± 0.0
18:4(*n*–3)	0.4 ± 0.5	4.4 ± 1.1	1.9 ± 0.6	3.7 ± 1.2	1.6 ± 0.1	3.0/1.3	1.1 ± 0.8	2.4 ± 0.2	1.7 ± 0.1	3.4 ± 0.4	5.1	4.7 ± 0.1
Phytanic acid	–	–	–	–	–	0.0/0.8	0.4 ± 0.7	0.4 ± 0.0	–	–	–	–
20:1(*n*–9)	1.7 ± 0.3	1.7 ± 1.9	0.2 ± 0.3	0.3 ± 0.5	0.4 ± 0.1	1.1/0.6	0.1 ± 0.2	–	0.5 ± 0.2	0.1 ± 0.3	0.7	1.8 ± 0.1
20:4(*n*–6)	8.7 ± 2.3	1.5 ± 0.2	1.6 ± 0.2	1.8 ± 0.4	0.9 ± 0.1	1.6/2.1	2.0 ± 0.4	3.3 ± 0.0	0.9 ± 0.0	3.4 ± 0.5	2.3	1.8 ± 0.0
20:5(*n*–3)	11.7 ± 0.7	14.0 ± 1.2	12.7 ± 0.3	15.6 ± 1.7	13.2 ± 0.4	10.2/10.7	14.4 ± 1.5	14.0 ± 0.1	9.6 ± 0.1	18.9 ± 0.9	18.2	15.3 ± 0.5
22:1(*n*–11)	–	4.1 ± 3.5	4.7 ± 0.8	1.6 ± 1.5	–	–	–	–	–	–	–	2.2 ± 0.3
22:6(*n*–3)	34.3 ± 2.8	33.1 ± 0.6	34.6 ± 1.2	32.7 ± 4.3	49.7 ± 0.9	33.6/28.4	30.0 ± 5.6	27.2 ± 1.8	47.7 ± 0.2	38.5 ± 1.6	36.9	25.0 ± 0.6
24:1(*n*–9)	–	1.8 ± 1.1	2.3 ± 0.1	1.9 ± 0.6	2.6 ± 0.6	2.6/3.1	2.7 ± 1.6	1.5 ± 0.3	1.7 ± 0.2	1.3 ± 0.0	–	0.9 ± 0.1
Carnivory index	0.63 ± 0.02	0.23 ± 0.07	0.27 ± 0.01	0.21 ± 0.06	0.38 ± 0.01	0.46/0.49	0.32 ± 0.07	0.25 ± 0.00	0.72 ± 0.00	0.11 ± 0.02	0.09	0.20 ± 0.00
Fatty alcohols (% TFAlc)												
14:0	–	3.5 ± 1.1	3.4 ± 0.1	7.0 ± 2.3	–	–	–	–	4.5 ± 0.2	–	–	8.6 ± 0.6
16:0	–	17.3 ± 3.5	13.0 ± 0.9	25.4 ± 7.8	–	–	–	–	89.7 ± 0.6	–	–	23.3 ± 0.6
16:1	–	2.9 ± 1.8	3.4 ± 0.6	8.0 ± 2.4	–	–	–	–	–	–	–	7.1 ± 0.2
18:0	–	3.4 ± 0.8	2.6 ± 0.2	3.9 ± 1.1	–	–	–	–	5.7 ± 0.6	–	–	3.5 ± 0.1
18:1(*n*–7)	–	1.3 ± 0.6	1.3 ± 0.1	2.6 ± 1.0	–	–	–	–	–	–	–	2.0 ± 0.0
18:1(*n*–9)	–	3.4 ± 0.9	2.8 ± 0.3	5.1 ± 1.3	–	–	–	–	–	–	–	3.8 ± 0.1
20:1	–	18.9 ± 3.8	18.3 ± 0.5	13.1 ± 1.9	–	–	–	–	–	–	–	14.2 ± 0.4
22:1	–	49.4 ± 5.6	55.2 ± 1.7	35.4 ± 10.4	–	–	–	–	14.7 ± 0.3	–	–	37.6 ± 0.8

(Continued)

TABLE 2 | (Continued)

	Euphausiacea					Decapoda				Peracarida
	E. distinguenda **f**	***E. eximia*** **f**	***E. mucronata*** **f**	***N. flexipes*** **f**	***Nematoscelis* sp.** **f**	***Acanthephyra* sp.** **f**	***Gennadas* sp.** **f**	***P. monodon*** **juv**	**f**	***Gnathophausia* sp.** **f**
n (ind)	6	6	9	2	3	4	4	3 (5)	6	4
Dry mass (mg ind^{-1})	4.41 ± 0.85	13.28 ± 5.85	12.07 ± 5.18	3.35/9.34	4.85 ± 0.88	665.26 ± 319.02	88.16 ± 16.25	3.54 ± 0.70	234.13 ± 47.34	406.71 ± 51.39
Total lipid (% DM)	12.1 ± 2.7	8.6 ± 1.8	11.3 ± 2.6	9.6/12.0	13.6 ± 7.7	42.2 ± 5.1	31.3 ± 17.7	15.2 ± 2.0	15.6 ± 4.1	47.8 ± 2.1
Wax esters (% TL)	–	–	–	9.7/26.9	–	70.3 ± 3.6	52.0 ± 25.9	–	–	75.3 ± 6.1
Fatty acids (% TFA)										
14:0	4.7 ± 2.4	3.5 ± 1.2	4.1 ± 1.5	2.5/1.2	2.3 ± 0.6	0.4 ± 0.2	0.5 ± 0.1	3.5 ± 0.1	3.8 ± 0.5	0.5 ± 0.1
16:0	17.5 ± 0.9	16.3 ± 0.9	16.4 ± 1.7	15.9/13.4	21.9 ± 3.5	3.6 ± 0.7	8.9 ± 3.8	18.4 ± 1.4	16.8 ± 0.8	2.9 ± 1.1
16:1(*n*–7)	3.9 ± 1.1	3.7 ± 1.6	4.4 ± 1.8	2.3/3.9	2.0 ± 1.4	9.1 ± 0.9	2.8 ± 0.6	6.7 ± 1.1	7.9 ± 0.7	11.5 ± 1.2
16:4(*n*–1)	0.3 ± 0.3	0.2 ± 0.3	0.6 ± 0.4	–	–	0.6 ± 0.6	0.3 ± 0.3	0.2 ± 0.1	1.6 ± 0.5	0.2 ± 0.3
18:0	2.6 ± 0.5	2.3 ± 0.3	2.0 ± 0.3	1.8/1.6	2.5 ± 0.3	0.9 ± 0.1	1.6 ± 0.3	3.6 ± 0.3	2.9 ± 0.3	0.8 ± 0.2
18:1(*n*–7)	3.9 ± 0.5	2.7 ± 0.7	3.4 ± 0.4	2.3/2.3	1.9 ± 0.4	2.8 ± 0.1	2.7 ± 0.4	4.3 ± 0.4	4.5 ± 0.5	3.1 ± 0.5
18:1(*n*–9)	8.8 ± 1.2	8.3 ± 1.3	8.3 ± 2.3	14.7/20.1	14.4 ± 4.2	60.0 ± 3.1	49.3 ± 2.2	10.4 ± 1.2	10.3 ± 0.8	53.8 ± 2.9
18:2(*n*–6)	3.1 ± 0.4	2.7 ± 0.4	2.5 ± 0.5	2.0/1.9	2.0 ± 0.6	0.7 ± 0.1	0.6 ± 0.1	1.5 ± 0.1	1.2 ± 0.4	0.9 ± 0.1
18:4(*n*–)	1.5 ± 0.4	1.6 ± 0.4	3.7 ± 1.2	0.7/0.8	1.3 ± 0.3	0.4 ± 0.3	0.2 ± 0.2	2.5 ± 0.3	2.6 ± 0.4	0.7 ± 0.1
Phytanic acid	–	–	–	–	–	0.1 ± 0.1	0.1 ± 0.2	1.0 ± 0.1	4.1 ± 0.7	0.2 ± 0.4
20:1(*n*–9)	0.7 ± 0.2	0.5 ± 0.3	0.6 ± 0.3	2.5/2.4	0.5 ± 0.4	2.1 ± 0.3	11.9 ± 1.2	1.4 ± 0.1	1.0 ± 0.2	5.8 ± 1.3
20:4(*n*–6)	4.2 ± 0.1	4.2 ± 0.6	3.2 ± 1.0	1.8/1.6	2.6 ± 0.6	1.0 ± 0.1	1.7 ± 0.3	1.6 ± 0.2	1.9 ± 0.4	1.3 ± 0.1
20:5(*n*–)	14.3 ± 1.1	14.7 ± 0.7	15.9 ± 1.8	11.4/11.7	14.3 ± 3.2	2.8 ± 0.6	2.6 ± 1.7	11.5 ± 1.4	16.9 ± 0.9	2.9 ± 1.7
22:1(*n*–11)	–	–	–	0.8/0.5	0.3 ± 0.4	–	0.1 ± 0.1	–	–	0.9 ± 0.2
22:6(*n*–)	26.3 ± 2.5	32.1 ± 3.4	27.0 ± 2.9	35.7/33.9	26.0 ± 11.3	11.2 ± 1.7	10.4 ± 2.5	24.5 ± 1.6	12.6 ± 2.1	6.9 ± 1.8
24:1(*n*–9)	–	–	–	0.3/0.0	0.9 ± 0.7	–	0.7 ± 0.1	0.3 ± 0.0	0.3 ± 0.1	–
Carnivory index	0.48 ± 0.07	0.51 ± 0.09	0.37 ± 0.06	0.73/0.74	0.72 ± 0.10	0.82 ± 0.02	0.89 ± 0.01	0.43 ± 0.01	0.38 ± 0.01	0.78 ± 0.01
Fatty alcohols (% TFAlc)										
14:0	–	–	–	0.0/2.9	–	1.1 ± 0.1	0.7 ± 1.0	–	–	6.5 ± 0.4
16:0	–	–	–	48.5/58.7	–	35.5 ± 2.5	23.1 ± 6.7	–	–	58.5 ± 4.9
16:1	–	–	–	–	–	2.3 ± 0.2	–	–	–	10.2 ± 0.4
18:0	–	–	–	11.0/7.7	–	10.1 ± 0.6	8.4 ± 3.3	–	–	5.1 ± 3.0
18:1(*n*–7)	–	–	–	–	–	5.4 ± 0.3	5.1 ± 3.1	–	–	1.5 ± 0.2
18:1(*n*–9)	–	–	–	0.0/4.2	–	18.2 ± 0.5	8.2 ± 3.3	–	–	15.7 ± 0.5
20:1	–	–	–	9.8/6.2	–	12.1 ± 1.4	44.4 ± 20.8	–	–	2.3 ± 2.1
22:1	–	–	–	30.7/20.4	–	15.4 ± 1.9	10.2 ± 6.1	–	–	0.2 ± 0.3

(Continued)

TABLE 2 | (Continued)

	Chaetognatha		Amphipoda		Thaliacea			Fishes		
	***Eukrohnia* sp.**	**Sagittidae**	**Gammaridae**	**Hyperiidae**	**Colonial salps**	***I. cylindrica***	***Pyrosoma* sp.**	***Cyclothone* sp.**	***E. ringens***	***S. chilensis***
n (ind)	3	3	3 (6)	3 (5)	3 (6)	2 (6)	3	3	3	3
Dry mass (mg ind^{-1})	5.47 ± 1.96	8.13 ± 3.85	2.86 ± 1.93	12.63 ± 2.53	86.13 ± 16.03	61.77 ± 33.06	99.75 ± 20.70	N.A.	N.A.	N.A.
Total lipid (% DM)	16.7 ± 3.7	4.7/11.2	17.5 ± 10.0	6.9 ± 0.3	1.4 ± 0.1	2.2 ± 3.3	2.4 ± 0.3	15.21 ± 5.6	19.9 ± 9.3	5.6 ± 3.5
Wax esters (% TL)	48.1 ± 14.0	-	–	8.4 ± 2.0	–	–	–	30.3 ± 12.0	–	–
Fatty acids (% TFA)										
14:0	0.7 ± 0.3	1.6 ± 0.9	2.4 ± 1.1	2.6 ± 0.5	4.5 ± 0.8	6.4/6.0	4.9 ± 1.8	1.1 ± 0.6	1.2 ± 0.4	2.3 ± 0.3
16:0	7.4 ± 3.3	12.9 ± 0.9	11.1 ± 0.3	15.8 ± 0.9	12.3 ± 0.2	12.1/12.1	17.7 ± 7.9	12.4 ± 1.4	14.2 ± 0.9	14.5 ± 0.7
16:1(*n*–7)	12.7 ± 1.5	6.8 ± 0.4	2.1 ± 0.5	1.8 ± 0.4	3.3 ± 0.3	2.5/2.6	3.2 ± 0.4	8.2 ± 1.7	1.1 ± 1.9	6.6 ± 3.0
16:4(*n*–1)	0.3 ± 0.3	–	–	–	0.5 ± 0.0	–	–	0.5 ± 0.3	0.9 ± 0.1	0.6 ± 0.2
18:0	1.8 ± 0.6	4.0 ± 0.3	2.9 ± 0.6	2.9 ± 0.3	2.5 ± 0.1	3.0/2.8	2.7 ± 2.4	4.0 ± 0.8	5.5 ± 1.1	2.7 ± 0.8
18:1(*n*–7)	2.4 ± 0.6	1.4 ± 0.2	1.2 ± 0.5	1.3 ± 0.2	1.0 ± 0.1	0.6/0.6	1.1 ± 0.4	1.9 ± 0.1	2.7 ± 0.1	2.4 ± 0.1
18:1(*n*–9)	39.0 ± 8.2	5.0 ± 0.6	7.2 ± 0.8	14.6 ± 2.1	3.0 ± 0.2	2.9/2.5	5.9 ± 1.4	30.1 ± 2.3	5.9 ± 0.6	12.5 ± 1.6
18:2(*n*–6)	0.7 ± 0.2	2.1 ± 0.3	1.8 ± 0.4	0.9 ± 0.2	2.1 ± 0.0	1.5/1.5	2.5 ± 0.9	0.9 ± 0.2	1.0 ± 0.2	1.0 ± 0.1
18:4(*n*–)	–	0.2 ± 0.2	3.8 ± 2.3	0.2 ± 0.3	6.7 ± 0.2	4.4/4.9	3.2 ± 0.8	0.4 ± 0.3	1.8 ± 0.1	1.8 ± 0.4
Phytanic acid	–	0.3 ± 0.6	–	–	–	–	–	–	–	–
20:1(*n*–9)	1.6 ± 0.4	1.0 ± 0.9	0.6 ± 0.3	1.2 ± 0.2	0.4 ± 0.0	0.5/0.4	–	1.0 ± 0.3	0.3 ± 0.5	0.7 ± 0.2
20:4(*n*–6)	1.5 ± 0.4	3.7 ± 0.1	4.0 ± 0.9	3.4 ± 0.1	2.3 ± 0.1	3.3/2.8	4.1 ± 1.6	2.2 ± 0.4	4.9 ± 0.9	1.9 ± 0.3
20:5(*n*–)	4.4 ± 0.7	15.0 ± 0.5	13.4 ± 0.3	10.2 ± 1.1	17.1 ± 0.1	12.3/11.7	6.6 ± 2.8	5.3 ± 0.4	18.9 ± 1.4	8.8 ± 0.7
22:1(*n*–11)	1.1 ± 0.3	–	–	–	0.5 ± 0.1	0.5/0.5	1.1 ± 0.5	1.3 ± 1.0	–	–
22:6(*n*–)	19.1 ± 1.6	36.9 ± 2.5	39.0 ± 1.3	40.6 ± 0.9	34.1 ± 0.6	40.7/41.3	32.1 ± 12.7	23.8 ± 3.8	31.4 ± 1.2	36.0 ± 3.8
24:1(*n*–9)	1.3 ± 0.2	3.7 ± 0.7	–	–	–	–	–	1.6 ± 0.5	1.8 ± 0.3	0.6 ± 0.4
Carnivory index	0.71 ± 0.06	0.37 ± 0.02	0.51 ± 0.09	0.81 ± 0.03	0.21 ± 0.01	0.28/0.24	0.44 ± 0.01	0.73 ± 0.02	0.48 ± 0.08	0.53 ± 0.05
Fatty alcohols (% TFAlc)										
14:0	6.2 ± 0.4	–	–	–	–	–	–	7.0 ± 1.3	–	–
16:0	60.4 ± 2.8	–	–	58.4 ± 1.4	–	–	–	60.7 ± 5.1	–	–
16:1	3.3 ± 0.9	–	–	–	–	–	–	–	–	–
18:0	3.5 ± 0.4	–	–	12.0 ± 0.3	–	–	–	6.9 ± 0.3	–	–
18:1(*n*–7)	6.3 ± 2.0	–	–	–	–	–	–	3.1 ± 2.4	–	–
18:1(*n*–9)	7.4 ± 3.8	–	–	10.8 ± 0.9	–	–	–	11.4 ± 4.7	–	–
20:1	7.1 ± 4.8	–	–	18.9 ± 1.6	–	–	–	–	–	–
22:1	5.8 ± 2.2	–	–	–	–	–	–	10.9 ± 8.8	–	–

All marker FAs and FAs with mean values >3% (group percentage) are presented. FA and FAlc compositions are shown as percentages of total fatty acids (% TFA) and total fatty alcohols (% TFAlc), wax esters in % of total lipid (% TL). Carnivory index (CI) = 18:1(n–9)/[Σ herbivory markers + 18:1(n–9)]. Σ herbivory markers: sum of 16:1(n–7), 16:4(n–1), 18:1(n–7), 18:4(n–3). n (ind), number of samples (total number of individuals); f: female; m: male; C5: copepodid 5; juv: juvenile. Taxa analyzed: Pterotrachea sp., Acartia sp., Centropages brachiatus, Calanus chilensis, Eucalanus inermis, Euchaeta rimana, Nannocalanus minor, Subeucalanus mucronatus, cyclopoid copepoda (cop.) bulk samples, Euphausia eximia, Euphausia distinguenda, Euphausia mucronata, Nematobranchion flexipes, Nematoscelis sp., Acanthephyra sp., Gennadas sp., Pleuroncodes monodon, Gnathophausia sp., Eukrohnia sp., Sagittidae, Gammaridae, Hyperiidae, colonial salps, Iasis cylindrica, Pyrosoma sp., Cyclothone sp., Engraulis ringens, Sarda chilensis.

euphausiids varied between 8.6 ± 1.8% DM in *E. eximia* and 13.6 ± 7.7% DM in *Nematoscelis* sp., while *E. mucronata* had lipid levels of 11.3 ± 2.6% DM. The peracarid *Gnathophausia* sp. and the decapods *Acanthephyra* sp. and *Gennadas* sp. had higher mean lipid levels between ∼31 and ∼48% DM, whereas the squat lobster *P. monodon* had lower lipid levels of 15.6 ± 4.1% DM (**Table 2**).

Fatty Acid and Fatty Alcohol Composition

Fatty acid compositions were taxon-specific and did not depend on sampling area or depth. Most species showed a dominance of typical membrane fatty acids (**Table 2** and **Figure 3**), e.g., 16:0, 20:5(*n*–3) and 22:6(*n*–3). In copepods, diatom marker FAs 16:1(*n*–7), 16:4(*n*–1), and 18:1(*n*–7) ranged between ∼3% of total fatty acids (TFA) in *E. rimana* and ∼11% TFA in female *Eucalanus inermis*, *S. mucronatus* and cyclopoids. In the dominant krill species *E. mucronata*, the diatom marker FA contribution was significantly higher with 9.0 ± 1.5% TFA compared to *Nematoscelis* sp. with 3.8 ± 0.9% TFA (Kruskal–Wallis test; Dunn's test, $H = 8.33$, df = 3, $p < 0.05$). The decapod *Gennadas* sp. had significantly lower mean levels of 16:1(*n*–7), 16:4(*n*–1), and 18:1(*n*–7) (5.8 ± 1.0% TFA) than *P. monodon* adults (14.0 ± 1.2% TFA) (Kruskal–Wallis test; Dunn's test, $H = 15.46$, df = 4, $p < 0.05$). The FA marker 18:4(*n*–3), indicative of dinoflagellates, generally occurred in low to moderate amounts (0.0–6.7% TFA). Thaliacea, except for *Pyrosoma* sp., were the group with the highest levels of the dinoflagellate marker (4.6–6.7% TFA). Among the krill species, *E. mucronata* had the highest levels of the dinoflagellate marker with 4.1 ± 1.0% TFA, significantly higher than in *Nematoscelis* sp. (Kruskal–Wallis test; Dunn's test, $H = 12.28$, df = 4, $p < 0.05$). Maximum concentrations of the monounsaturated marker FAs 20:1(*n*–9) and 22:1(*n*–11) synthesized *de novo* by calanid copepods were detected in the decapod *Gennadas* sp. (12.0 ± 1.2% TFA). In comparison, adult squat lobsters *P. monodon* had significantly lower levels of calanid copepod markers with 1.0 ± 0.2% TFA, (Kruskal–Wallis test; Dunn's test, $H = 19.10$, df = 4, $p < 0.05$). Zero to low calanid markers were detected in copepods, except for bulk samples of cyclopoids (∼4% TFA) and for *C. chilensis* (∼1.2–6.0% TFA). The carnivory marker 18:1(*n*–9) was highest in decapods (∼49–60% TFA), except for *P. monodon*, which only contained ∼10% TFA. The chaetognath *Eukrohnia* sp. showed a very high amount of this carnivory marker (∼39% TFA). Among the fish species, highest levels of the carnivory marker were determined in muscle tissue of the mesopelagic *Diogenichthys laternatus* (59.9% TFA) and for specimens of *Cyclothone* sp. (30.2 ± 2.8% TFA).

Among the eight copepod taxa investigated, three contained considerable amounts of fatty alcohols (mean values ≥10% of total lipid), indicating the storage of wax esters (**Table 2**). *C. chilensis*, *E. rimana* and the cyclopoid bulk samples exhibited moderate to high wax ester portions between 29.4 ± 0.4% TL (*E. rimana*) and 65.0 ± 2.7% TL (*C. chilensis* males). *C. chilensis* C5s and males contained significantly higher wax ester amounts (∼60% TL) than their female conspecifics with ∼40% TL (Mann–Whitney test, $p < 0.01$). The long-chain mono-unsaturated fatty alcohols (FAlcs) 20:1 and 22:1 (together >45% TFAlc) dominated in all stages of *C. chilensis* as well as in the cyclopoids, whereas the saturated FAlc 16:0 prevailed in *E. rimana* with ca. 90% TFAlc. Very high wax ester contents occurred in deep-sea decapods (ca. 65% TL) and the peracarid *Gnathophausia* sp. with 75% TL. In contrast, squat lobsters *P. monodon* did not accumulate wax esters. Within the group of chaetognaths, *Eukrohnia* sp. had wax ester levels of around 50% TL with high concentrations of the short-chain fatty alcohol 16:0 (∼60% TFAlc), whereas Sagittidae contained no fatty alcohols.

Although individuals were sampled across an extensive region and depth range, principal component analysis (PCA) based on FA compositions of crustaceans mostly grouped individuals of the same species closely together (**Figure 4**). The first two principal components (PCs) account for 66% of the variance among the crustaceans. PC1 is mainly represented by positive values for 18:1(*n*–9), 18:1(*n*–7) and phytanic acid and negative values for 22:6(*n*–3), 24:1(*n*–9), and 22:1(*n*–11) all listed in decreasing order of explanatory power. PC2 is characterized by positive values for 22:1(*n*–11), 16:1(*n*–7), and 16:4(*n*–1) and negative values for 22:6(*n*–3) and 18:1(*n*–9), again listed in decreasing order of explanatory value. The copepods *Nannocalanus minor* and *E. rimana* were characterized by very high amounts of 22:6(*n*–3) of ∼49% TFA. Different contributions of the carnivory marker 18:1(*n*–9) further distinguished the various copepod species: *S. mucronatus* C5 copepodids (4.4 ± 0.2% TFA), *E. inermis* (5–9% TFA) and *E. rimana* (11.2 ± 0.4% TFA) contained higher amounts of this carnivory marker FA than all other copepod species (usually well below 5% TFA). The euphausiids showed comparably high values of 18:1(*n*–9), ranging from 6–9% TFA in *E. mucronata* to 9–20% TFA in *Nematoscelis* sp. and *Nematobranchion flexipes*, which separated them from most copepods. The adult squat lobster *P. monodon* was distinguished from the euphausiids by the higher amounts of 16:1(*n*–7) and phytanic acid.

Carnivory Index

The carnivory index (CI, **Table 2**), based on the fatty acid ratio 18:1(*n*–9)/[16:1(*n*–7) + 16:4(*n*–1) + 18:1(*n*–7) + 18:4(*n*–3) + 18:1(*n*–9)], reflects the proportion of carnivorous compared to herbivorous feeding in an organism. An organism with a CI close to zero is predominantly herbivorous, whereas an organism with CI close to 1 is primarily carnivorous; values in between indicate different levels of omnivory. Copepods exhibited a wide range of CI values between 0.09 in *Acartia* sp. and 0.72 in *E. rimana*. *C. brachiatus*, cyclopoids and all stages of *C. chilensis* had mean CIs below 0.3, while *E. inermis* and *N. minor* ranged between 0.32 ± 0.07 and 0.46/0.49. With 0.37 ± 0.06, the dominant krill species *E. mucronata* showed a significantly lower CI than *Nematoscelis* sp. with 0.72 ± 0.10 (Kruskal–Wallis test; Dunn's test, $H = 12.8$, df = 3, $p < 0.01$). The squat lobster *P. monodon* had significantly lower ratios of carnivory with values of 0.43 ± 0.01 in juveniles and 0.38 ± 0.01 in adults compared to the deep-sea decapods *Gennadas* sp. and *Acanthephyra* sp. and the peracarid *Gnathophausia* sp. (Mann–Whitney test, $p < 0.001$) with means between 0.78 and 0.89. The chaetognath *Eukrohnia*

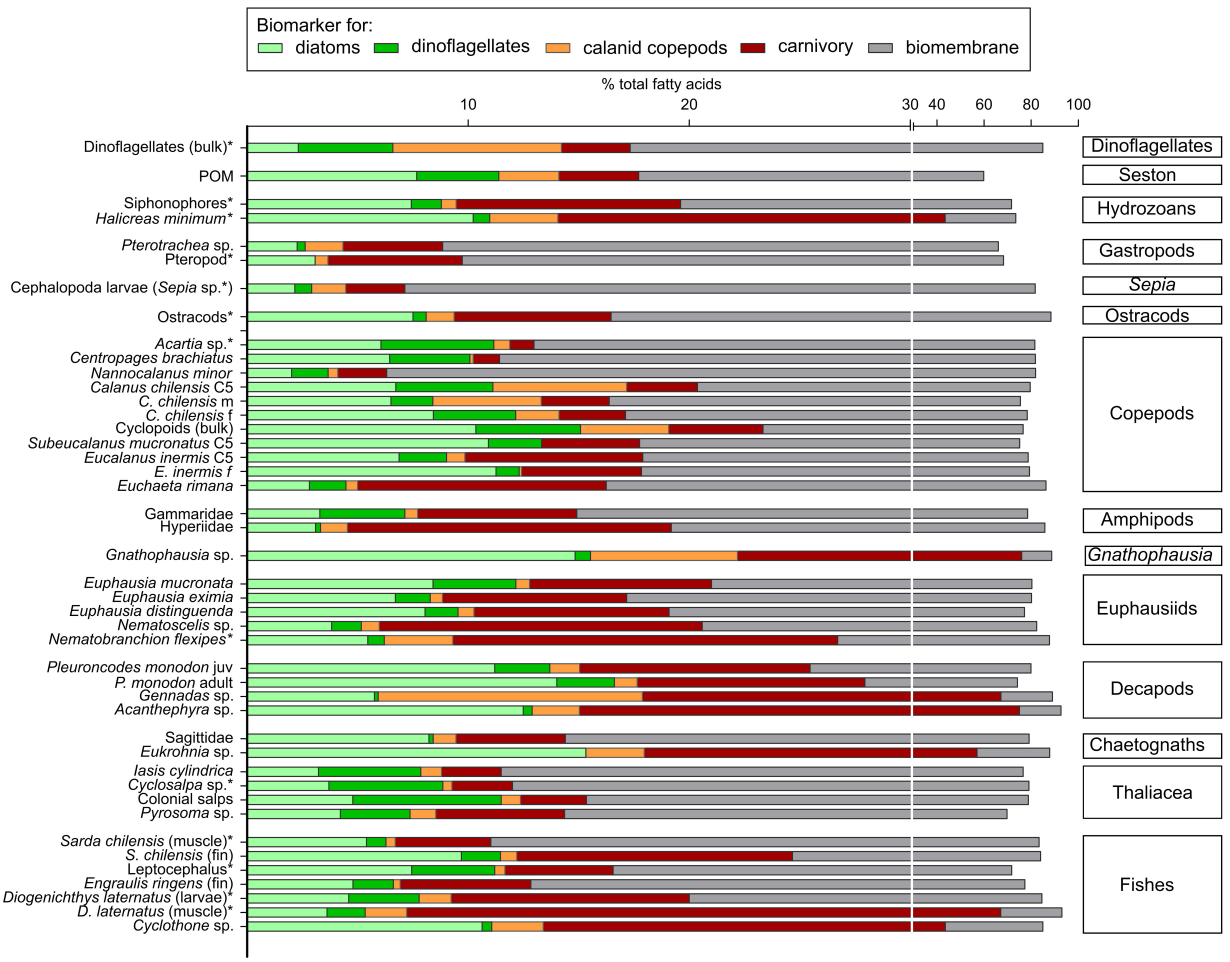

FIGURE 3 | Fatty acid biomarker compositions of plankton and nekton. Bars are divided into contributions of marker fatty acids for diatoms [16:1(*n*–7), 16:4(*n*–1), 18:1(*n*–7)] in light-green, dinoflagellates [18:4(*n*–3)] in dark-green, calanid copepods [20:1(*n*–9), 22:1(*n*–11)] in orange, carnivory [18:1(*n*–9)] in red, and typical fatty acids of biomembranes [16:0, 20:5(*n*–3), 22:6(*n*–3)] in gray. If $n \geq 3$, mean values are presented; taxa with asterisk: $n < 3$, measured value presented or mean value calculated from two measured values (note break in scale). Groups are sorted according to phylogeny; within each group, taxa are arranged by increasing amounts of carnivory marker fatty acid levels; different stages or tissues of the same species/genus are grouped together. C5: copepodid 5; f: females; m: males; juv: juveniles. Taxa with asterisk: $n < 3$.

sp. showed a much higher CI with 0.71 ± 0.06 than the other dominant chaetognath Sagittidae (0.37 ± 0.02). Within the group of Thaliacea, *Pyrosoma* sp. had a significantly higher CI of 0.44 ± 0.01 than salps with values ranging between 0.16 and 0.28 (Mann–Whitney test, $p < 0.05$). Among the fishes, the CI of the mesopelagic *Cyclothone* sp. ranked first with 0.73 ± 0.02. *Sarda chilensis* exhibited with 0.53 ± 0.05 slightly higher CIs than the anchovy *E. ringens* (0.48 ± 0.08).

Stable Isotope Ratios ($\delta^{13}C$ and $\delta^{15}N$)

Most samples for stable isotope analysis were collected in the northern part of the investigation area from 8.5 to 10.5°S. The ratios of $\delta^{15}N$ and $\delta^{13}C$' for this region are shown in **Figure 5** for surface (100/50–0 m) and deeper layers (600–200 m) within the OMZ. In general, low isotope ratios at the surface occurred in Thaliacea (*I. cylindrica* and *Pyrosoma* sp.) and POM ($\delta^{15}N$: ca. 2–6‰; $\delta^{13}C$': ca. −23 to −20‰). *I. cylindrica* $\delta^{15}N$ ratios at stns. 7, 15, and 18 were comparable or slightly higher than the corresponding POM values, while $\delta^{15}N$ at stn. 4 was ∼2‰ higher for the salps than for POM. $\delta^{15}N$ values of copepods inhabiting waters <50 m depth ranged from 3.9 ± 0.2‰ in *N. minor* to 6.7 ± 0.6‰ in *C. chilensis*. $\delta^{13}C$' mean values of these copepods varied greatly from -21.3 to −17.4‰. Intraspecific differences in $\delta^{13}C$' ratios were detected between stations: The copepod *C. chilensis* had a higher value of −17.4‰ at the coast (**Figure 5A**, turquoise) compared to its offshore conspecifics with −19.8‰ (**Figure 5A**, orange). For the diel vertical migrating euphausiids, mean $\delta^{15}N$ (5.1–7.7‰) and $\delta^{13}C$' values (−21.2 to −19.1‰) were in a similar range as for copepods from the upper water layers. $\delta^{15}N$ of the squat lobster *P. monodon* (7.8 ± 0.7‰) was comparable to that of the euphausiids, whereas the $\delta^{13}C$' ratios of *P. monodon* were extraordinarily high (−15.2 ± 0.6‰). Among the key fish species, the eastern Pacific bonito *Sarda chilensis* had a slightly

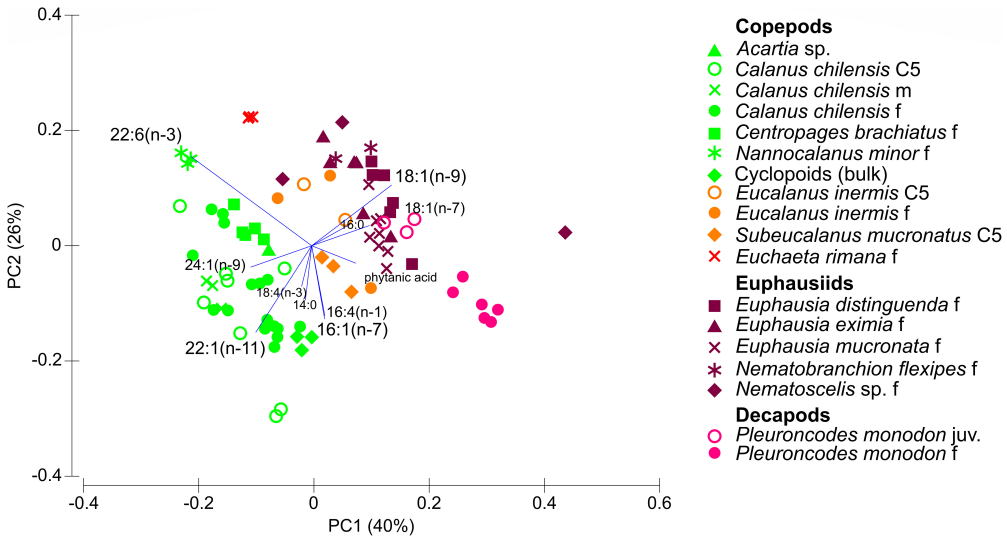

FIGURE 4 | Principal component analysis (PCA) based on fatty acid compositions of copepods, euphausiids and the decapod *P. monodon*. Taxa are arranged according to the first two principal components PC1 and PC2. C5: copepodid 5; f: females; m: males; juv: juveniles.

higher δ^{15}N value of 13.3 ± 1.2‰ compared to the anchovy *E. ringens* with 11.2 ± 0.2‰, but similar δ^{13}C' values of −16.4 to −16.6‰, respectively.

In contrast to the surface, mean δ^{15}N values for POM were 1.4–3.8‰ higher within the OMZ core, while δ^{13}C' values fell into a similar range within and above the OMZ. Deeper-living copepods (>200 m depth) within the OMZ core had about 4–8‰ higher δ^{15}N values (∼11–15‰) than surface living ones and only a small range in mean δ^{13}C' values (−20.0 and −19.1‰). δ^{15}N of deep-living decapods were lower (∼7.6–9.3‰) than those of the deep-sea copepods. The mesopelagic fish *Cyclothone* sp. was enriched in δ^{15}N (10.0‰; 11.4‰) and δ^{13}C' (−18.9‰; −18.4‰) as compared to the surface-dwelling anchovy and eastern Pacific bonito.

A strong regional shift in δ^{15}N values occurred in many taxa; values generally increased from the northern to the southern part of the study area (**Figures 2**, **6**). The increase in δ^{15}N ratios of ∼4–5‰ from Transect 1 (T1) in the North to T6 in the South was significant for the copepod species *N. minor*, *C. chilensis*, and *E. inermis* and for the euphausiid *E. mucronata* (Mann–Whitney test, $p < 0.01$). Despite the significant regional shift in δ^{15}N ratios, the organisms maintained their relative positions toward each other.

Regionally differentiated δ^{15}N ratios for more than 50 taxa from the base of the food web up to fish and seabirds are shown in **Figure 6**. Mean δ^{15}N varied greatly from 2.0‰ in salps and POM to 15.4‰ in deep-sea copepods, fish and storm petrels. The δ^{15}N values increased from the North to the South for all taxa investigated, except for the deep-sea copepod *Metridia* sp. and the seabirds. The copepods from the upper water layers covered the entire δ^{15}N range of the euphausiids and squat lobsters, whereas the deep-sea copepods exhibited the highest δ^{15}N of the investigated taxa from the OMZ, higher than the δ^{15}N values of POM, amphipods and decapods from the OMZ. The chaetognath Sagittidae from the upper water layers had similar values compared to the salp *I. cylindrica*, while the chaetognath from the OMZ, *Eukrohnia* sp., showed higher values, comparable to those of *Cyclothone* sp. and the deep-sea copepods. The Peruvian anchovy *E. ringens* had ∼1.5‰ lower δ^{15}N mean ratios compared to the eastern Pacific bonito *S. chilensis* in the central and southern investigation area.

Trophic positions calculated with either POM as reference for TP 1 or the salp *I. cylindrica* as reference for TP 2 are shown in **Table 3**. TPs calculated via *I. cylindrica* are presented in the following. The copepods *C. chilensis* (TP 1.8–2.6) and *N. minor* (TP 1.4–1.9) occupied low TPs, while *S. mucronatus* had more variable TPs between 2.1 and 3.1. Specimens of *E. inermis* occupied higher TPs (3.3–5.0) within the OMZ at depth of 600–200 m as compared to surface-dwelling individuals (TP 2.0 ± 0.3). Copepods from deeper water layers >500 m had similar high TPs (3.8–5.3) as *E. inermis* in the OMZ. The squat lobster *P. monodon* occupied a TP of 2.5 ± 0.3 as adults and 2.7 as zoea larvae ($n = 1$). Among the krill species, *E. mucronata* and *E. eximia* had TPs between 2.1 and 2.6. *Euphausia distinguenda* showed a high variation in TP, ranging from TP 2.2 ± 0.2 at transect 2 to TP 3.9/3.7 at transect 1. *N. flexipes* and *Nematoscelis* sp. showed TPs of 2.9–3.5. Adult *E. ringens* had a TP of 3.4 ± 0.1, while larvae occupied a lower TP of 2.4 ($n = 1$). TPs of adult *Sarda chilensis* were higher (∼4) than those of *E. ringens*.

DISCUSSION

Challenges in the Determination of Trophic Positions

We are aware that our data were obtained only from one expedition during one season (December 2018/January 2019). Therefore, inter-annual and seasonal variations cannot be

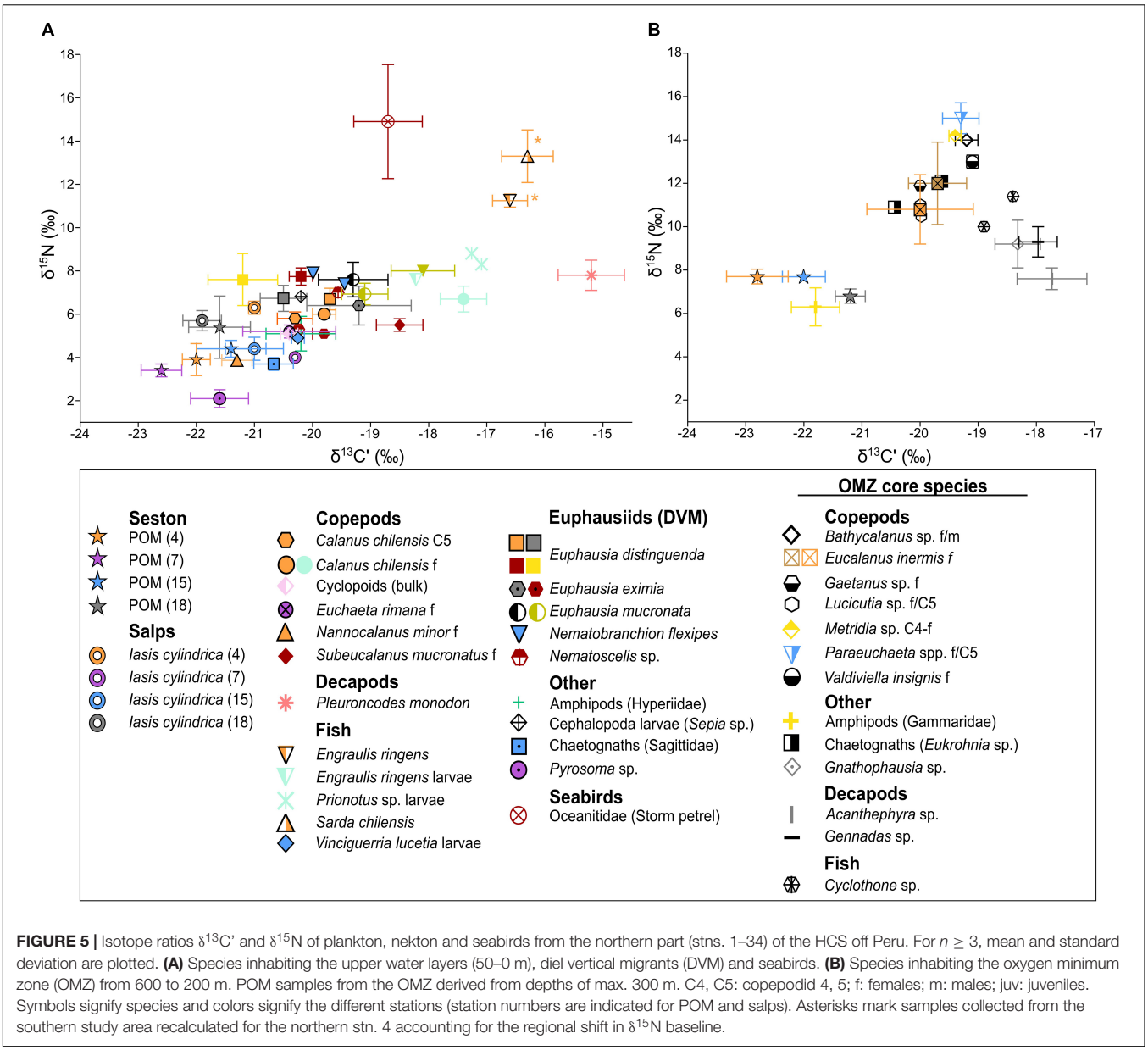

FIGURE 5 | Isotope ratios $\delta^{13}C'$ and $\delta^{15}N$ of plankton, nekton and seabirds from the northern part (stns. 1–34) of the HCS off Peru. For $n \geq 3$, mean and standard deviation are plotted. **(A)** Species inhabiting the upper water layers (50–0 m), diel vertical migrants (DVM) and seabirds. **(B)** Species inhabiting the oxygen minimum zone (OMZ) from 600 to 200 m. POM samples from the OMZ derived from depths of max. 300 m. C4, C5: copepodid 4, 5; f: females; m: males; juv: juveniles. Symbols signify species and colors signify the different stations (station numbers are indicated for POM and salps). Asterisks mark samples collected from the southern study area recalculated for the northern stn. 4 accounting for the regional shift in $\delta^{15}N$ baseline.

detected by our dataset alone. Trophic positions may shift due to different environmental conditions such as the availability of prey or different sources of primary production (e.g., Castro et al., 2020).

Baseline Shifts Due to Nitrogen Dynamics

$\delta^{15}N$ isotope ratios provide integrated dietary information and can therefore be used to reveal trophic roles and positions of organisms within the food web. In contrast to the fatty acid signals, substantial regional differences in $\delta^{15}N$ values occurred over the extended study area, with an overall tendency of higher isotope ratios toward the southern region (~14–16°S). In some species, such as the key copepod *C. chilensis,* a strong increase of the $\delta^{15}N$ ratio of up to ~5‰ was determined from North (8.5°S) to South (16°S), resulting in high $\delta^{15}N$ of ~11‰ for this species in the South. The key krill species *E. mucronata* increased by ~4‰ in mean $\delta^{15}N$ ratios from the northernmost to the southernmost transect. A similar increasing gradient of $\delta^{15}N$ values for higher trophic position organisms (i.e., fish and squid) from 5°S to 15°S was observed by Espinoza et al. (2017). The strong spatial differences in $\delta^{15}N$ values between conspecifics indicate a substantial shift in $\delta^{15}N$ baseline ratios.

Such baseline shifts are apparently caused by different nitrogen dynamics that are driven by the shallow and pronounced OMZ in the northern HCS (Chavez and Messié, 2009). OMZs like the one in the northern HCS are sites of intense nitrogen loss, which leads to an enrichment of $\delta^{15}N$ baseline values (Sigman et al., 1999; Graham et al., 2010). Denitrification within the OMZ causes isotopic fractionation where isotopically lighter nitrate ($\delta^{14}N$) is respired by bacteria leaving behind subsurface nitrate

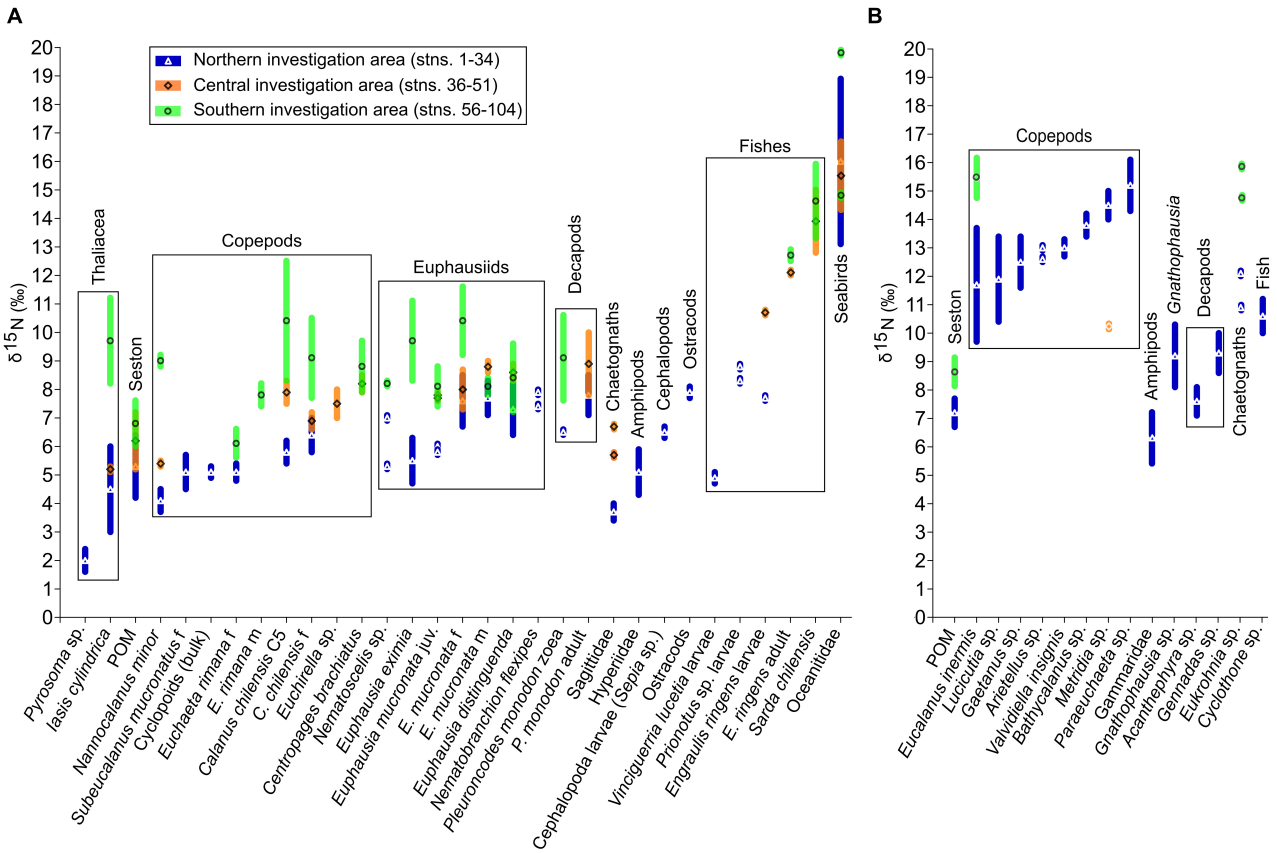

FIGURE 6 | Regional differences in $\delta^{15}N$ ratios of plankton, nekton and seabirds of the HCS off Peru. Sampling regions are color- and symbol-coded. For $n \geq 3$, mean and standard deviation are plotted. **(A)** Species generally inhabiting the upper water layers (50–0 m), diel vertical migrants and seabirds. **(B)** Species inhabiting the oxygen minimum zone (OMZ) from 600 to 200 m. Copepods and decapods are adult females (f), unless indicated otherwise. C5: copepodid 5; f: females; m: males; juv: juveniles; stns.: stations.

enriched in $\delta^{15}N$. This nitrate with higher $\delta^{15}N$ values is upwelled to the surface, where it is taken up by phytoplankton and passed on through the food web to higher trophic levels (Mollier-Vogel et al., 2012; Doering et al., 2019). The intensified oxygen depletion from North to South in the northern HCS provides evidence for the strongest denitrification rates that have been previously reported from the south (Fuenzalida et al., 2009; Bertrand et al., 2010; Espinoza et al., 2017). Our results suggest that oxygen dynamics are the primary driver for the pronounced latitudinal differences in $\delta^{15}N$ values in the northern HCS off Peru.

Additionally, preferential uptake of NO_3^- containing lighter $\delta^{14}N$ by phytoplankton in surface waters results in progressive enrichment of $\delta^{15}N$ in left over nitrate (Granger et al., 2009; Mollier-Vogel et al., 2012). Phytoplankton takes up the remaining $\delta^{15}N$ enriched NO_3^-, thus propagating the signal along the food web (Mollier-Vogel et al., 2012). Surface depletion in inorganic nutrients was observed on Transects 5 and 6 in the South (Kastriot Qelaj, pers. comm., Geomar Helmholtz Centre for Ocean Research, Kiel), which coincides with maximum $\delta^{15}N$ values measured. Therefore, phytoplankton in this region may have already consumed enriched NO_3^-, resulting in a baseline with higher $\delta^{15}N$ values. These complex nitrogen dynamics complicate the interpretation of $\delta^{15}N$ data over larger spatial scales in a highly variable system such as the HCS.

The pronounced differences in $\delta^{15}N$ values between northern, central and southern regions of the HCS off Peru highlight the importance of adequate baseline values to avoid misinterpretations of the species' regional feeding behavior. In fact, calculated trophic positions for *C. chilensis* and other species did not differ between regions, when shifts in the baseline were taken into account. Hence, we accept our first hypothesis of pronounced regional shifts in the $\delta^{15}N$ baseline of the food web from North to South.

A promising approach for future research in such highly dynamic systems is the compound-specific isotope analysis of amino acids (CSIA-AA) that allows to distinguish between variations in isotope ratios caused by baseline shifts and heterogeneity due to changes in feeding behavior (e.g., Hannides et al., 2009; Larsen et al., 2013; Hetherington et al., 2017). The difference in $\delta^{15}N$ enrichment of source amino acids and trophic amino acids may lead to a more precise determination of trophic positions without the need for an independent baseline determination (e.g., McClelland and Montoya, 2002; Chikaraishi et al., 2009; Hetherington et al., 2017). Current studies work

TABLE 3 | Stable isotope ratios ($\delta^{15}N$ and $\delta^{13}C'$) and trophic positions (TP) of pelagic species from the northern HCS.

Species	Stage	*n* (ind)	Depth (m)	Station		$\delta^{13}C$ (‰)	$\delta^{13}C'$ (‰)	$\delta^{15}N$ (‰)	*C:N*	TP (I)	TP (P)
Surface species											
Copepoda											
Calanus chilensis	C5	7 (87)	50–0	4	T1	−21.3 ± 0.4	−20.3 ± 0.4	5.8 ± 0.4	5.2 ± 0.3	1.8 ± 0.1	1.5 ± 0.1
	C5	1 (6)	50–0	80	T5	−18.7	−18.2	8.4	4.5	2.2	1.7
	C5	3 (17)	50–0	102	T6	−19.5 ± 0.3	−19.2 ± 0.3	12.4 ± 0.5	4.3 ± 0.1	2.6 ± 0.1	2.2 ± 0.1
	f	7 (60)	50–0	4	T1	−20.4 ± 0.5	−19.8 ± 0.2	6.0 ± 0.2	4.6 ± 0.4	1.9 ± 0.1	1.6 ± 0.1
	f	3 (17)	50–0	80	T5	−18.1 ± 0.1	−18.1 ± 0.1	7.7 ± 0.1	4.6 ± 0.0	2.0 ± 0.0	1.3 ± 0.0
	f	3 (21)	50–0	102	T6	−20.6 ± 0.2	−20.1 ± 0.3	10.8 ± 0.2	4.5 ± 0.3	2.2 ± 0.0	1.7 ± 0.0
Nannocalanus minor	f	8 (97)	50–0	4 + 7	T1	−21.2 ± 0.4	−21.1 ± 0.4	4.1 ± 0.4	4.1 ± 0.1	1.9 ± 0.2	1.4 ± 0.1
	f	4 (40)	50–0	99	T6	−21.7 ± 0.1	−21.6 ± 0.2	9.0 ± 0.2	4.0 ± 0.0	1.4 ± 0.1	1.3 ± 0.1
	m	1 (12)	20–0	7	T1	−20.8	−20.7	4.4	4.1	2.1	1.3
Subeucalanus mucronatus	f	3 (12)	50–0	1	T1	−19.0 ± 0.4	−18.5 ± 0.4	5.5 ± 0.3	4.5 ± 0.1	3.1 ± 0.1	1.9 ± 0.1
	f	2 (7)	50–0	7	T1	−22.5/−20.2	−22.4/−19.9	4.4/4.4	4.1/4.3	2.1/2.1	1.3/1.3
Euchaeta rimana	f	2 (7)	50–0	1	T1	−20.6/−21.1	−20.2/−20.5	4.8/4.4	4.4/4.6	2.8/2.7	1.6/1.5
	f	8 (18)	50–0	7	T1	−21.3 ± 0.3	−20.4 ± 0.8	5.2 ± 0.3	5.4 ± 1.7	2.4 ± 0.1	1.8 ± 0.1
Centropages brachiatus	f	1 (14)	50–0	80	T5	−18.9	−18.3	8.2	4.6	2.1	1.4
	f	4 (70)	100–0	40	T3	−17.7 ± 0.2	−17.2 ± 0.1	7.9 ± 0.1	4.5 ± 0.1	n.d.	1.4 ± 0.0
	f	5 (83)	50–0	51		−16.9 ± 0.4	−16.5 ± 0.3	8.4 ± 0.1	4.5 ± 0.1	n.d.	1.3 ± 0.0
Labidocera sp.	m	1	50–0	18	T2	−19.9	−19.7	6.6	4.2	2.3	1.4
Acartia sp.	C4–6	2 (–)	20–0	67	T5	−19.0/−19.2	−18.3/−18.6	7.6/7.0	4.7/4.6	n.d.	0.8/0.6
Amphipoda (hyperiid)		3	90–50	25	T2	−21.1 ± 0.6	−20.2 ± 0.6	5.1 ± 0.8	5.0 ± 0.2	n.d.	0.8 ± 0.3
Appendicularia		1 (3)	50–0	4	T1	−21.3	−21.0	3.9	4.3	1.3	1.0
		2 (38)	50–0	56	T4	−22.7/−22.8	−22.7/−22.7	2.8/2.9	4.0/4.1	n.d.	−0.3/−0.3
Chaetognatha (sagittidae)		3	50–0	15		−20.8 ± 0.3	−20.7 ± 0.3	3.7 ± 0.3	4.1 ± 0.0	1.8 ± 0.1	0.8 ± 0.1
Fish											
Bisigeria sp.	Larvae	3	50–0	15		−20.6 ± 0.2	−20.3 ± 0.1	4.9 ± 0.2	4.3 ± 0.1	2.2 ± 0.1	1.2 ± 0.1
Engraulis ringens	Larvae	1	30–0	4	T1	−18.8	−18.2	7.7	4.6	2.4	2.1
	Adult	5	350–0	4*	T1	−16.6 ± 0.2	−16.6 ± 0.1	11.2 ± 0.2*	4.0 ± 0.1	3.4 ± 0.1*	3.1 ± 0.1*
	Adult	3	350–0	68	T5	−16.6 ± 0.2	−16.6 ± 0.1	12.6 ± 0.2	4.0 ± 0.0	n.d.	3.0 ± 0.1
Sarda chilensis	Adult	6	10–0	4*	T1	−16.3 ± 0.4	−16.4 ± 0.3	13.1 ± 1.2*	3.9 ± 0.1	4.0 ± 0.4*	3.7 ± 0.4*
	Adult	3	10–0	46	T3	−16.4 ± 0.1	−16.4 ± 0.2	13.9 ± 1.1	3.9 ± 0.1	n.d.	3.3 ± 0.3
	Adult	3	10–0	80	T5	−16.6 ± 0.6	−16.6 ± 0.4	14.1 ± 1.4	4.0 ± 0.2	3.9 ± 0.4	3.1 ± 0.4
Diel vertical migrants											
Euphausiacea											
Euphausia distinguenda	f	2	200–0	1	T1	−20.6/−20.2	−20.4/−20.1	7.3/7.4	4.2/4.1	3.6/3.6	2.6/2.6
	f	2	600–400	1	T1	−21.0/−20.6	−20.4/−20.0	8.4/7.9	4.7/4.6	3.9/3.7	2.7/2.5
	f	6	500–200	4 + 18	T2	−20.5 ± 0.5	−20.1 ± 0.5	6.7 ± 0.6	4.4 ± 0.1	2.2 ± 0.2	1.6 ± 0.3
	f	2	400–200	80	T5	−19.4/−19.4	−18.9/−19.0	10.1/9.5	4.5/4.3	2.7/2.5	2.0/1.8
Euphausia eximia	f	3	30–0	1	T1	−20.0 ± 0.3	−19.8 ± 0.2	5.1 ± 0.2	4.2 ± 0.1	2.9 ± 0.1	1.7 ± 0.1
	f	3	500–200	18	T2	−19.8 ± 0.7	−19.3 ± 0.8	5.9 ± 1.0	4.5 ± 0.1	2.1 ± 0.3	1.2 ± 0.3
Euphausia mucronata	juv	2	400–200	80	T5	−18.9/−19.0	−18.0/−18.1	8.2/8.7	5.0/5.0	2.1/2.3	1.7/1.8
	f	7	500–200	4	T1	−20.5 ± 0.3	−20.1 ± 0.2	7.5 ± 0.7	4.4 ± 0.1	2.4 ± 0.2	2.0 ± 0.2
	f	8	400–200	80	T5	−18.9 ± 0.3	−18.2 ± 0.3	9.8 ± 0.4	4.7 ± 0.1	2.6 ± 0.1	1.9 ± 0.1
	f	3	500–200	102	T6	−19.3 ± 0.5	−18.4 ± 0.4	11.6 ± 1.3	4.9 ± 0.1	2.4 ± 0.4	2.0 ± 0.4
Nematobranchion flexipes	f	2	100–0	15		−20.1/−20.1	−19.4/−20.0	7.4/7.9	4.7/4.1	2.9/3.0	1.9/2.0
Nematoscelis sp.	f	2	200–0	1	T1	−20.4/−20.0	−20.2/−19.6	5.3/7.0	4.1/4.4	3.0/3.5	1.8/2.3
Decapoda											
Pleuroncodes monodon	Zoea	1 (10)	50–20	7	T1	−17.5	−16.5	6.5	5.2	2.7	1.9
	Zoea	3 (8)	50–0	74	T5	−19.5 ± 0.1	−18.2 ± 0.2	7.8 ± 0.1	5.6 ± 0.1	n.d.	1.4 ± 0.0
	Zoea	3 (30)	50–0	104	T6	−20.3 ± 0.2	−19.4 ± 0.2	10.9 ± 0.1	5.0 ± 0.1	n.d.	1.6 ± 0.0.
	Adult	6	50–0	4*	T1	−16.0 ± 0.4	−14.9 ± 0.7	8.1 ± 0.9*	5.3 ± 0.6	2.5 ± 0.3*	2.2 ± 0.3*
	Adult	3	50–0	30	T2	−16.3 ± 0.2	−15.2 ± 0.6	7.8 ± 0.7	5.4 ± 0.6	n.d.	1.4 ± 0.2
	Adult	3	50–0	40	T3	−15.8 ± 0.4	−14.7 ± 0.7	8.9 ± 1.1	5.3 ± 0.5	n.d.	1.5 ± 0.3

(Continued)

TABLE 3 | (Continued)

Species	Stage	*n* (ind)	Depth (m)	Station		$\delta^{13}C$ (‰)	$\delta^{13}C'$ (‰)	$\delta^{15}N$ (‰)	*C:N*	TP (I)	TP (P)
Acanthephyra sp.		4	1000–0	18	T2	−19.0 ± 0.5	−17.7 ± 0.6	7.6 ± 0.5	5.6 ± 0.1	2.5 ± 0.2	1.6 ± 0.2
Gennadas sp.		3	1000–0	31		−19.0 ± 0.4	−18.0 ± 0.3	9.3 ± 0.7	5.2 ± 0.1	n.d.	2.2 ± 0.2
Peracarida											
Gnathophausia sp.		4	1000–0	18	T2	−19.2 ± 0.4	−18.3 ± 0.4	9.2 ± 1.1	4.9 ± 0.3	3.0 ± 0.3	2.1 ± 0.3
OMZ residents											
Copepoda											
Eucalanus inermis	C5	4 (10)	100–50	4	T1	−21.5 ± 0.3	−20.9 ± 0.2	9.5 ± 0.4	4.6 ± 1.8	3.0 ± 0.1	2.6 ± 0.1
	f	6	600–200	1	T1	−20.2 ± 0.6	−19.7 ± 0.5	12.0 ± 1.9	4.6 ± 0.5	5.0 ± 0.6	3.8 ± 0.6
	f	6 (10)	500–200	4	T1	−20.3 ± 0.8	−20.0 ± 1.3	10.8 ± 1.6	4.4 ± 0.7	3.3 ± 0.5	3.0 ± 0.5
	f	7	50–0	99	T6	−21.4 ± 0.2	−20.6 ± 0.2	10.3 ± 1.0	4.9 ± 0.7	2.0 ± 0.3	2.1 ± 0.3
	f	5	500–200	104	T6	−20.2 ± 0.4	−18.9 ± 0.5	15.2 ± 0.7	5.7 ± 0.6	n.d.	2.9 ± 0.2
Gaetanus sp.	C4–C5	2 (3)	1000–500	15		−21.8/−22.8	−20.1/−19.3	11.9/13.8	6.4/11.5	4.2/4.8	3.2/3.8
Lucicutia sp.	C5, f	2	1000–500	15		−21.3/−22.2	−19.9/−20.0	10.5/11.1	5.8/7.9	3.8/4.0	2.8/3.0
Paraeuchaeta spp.	C4–5	8	1000–500	15		−21.0 ± 1.5	−19.0 ± 0.6	15.4 ± 1.0	8.1 ± 2.6	5.2 ± 0.3	4.2 ± 0.3
Paraeuchaeta spp.	f	3	1000–500	1 + 15		−22.1 ± 0.3	−19.3 ± 0.4	14.9 ± 0.7	10.1 ± 0.6	5.3 ± 0.2	4.3 ± 0.1
Amphipoda (gammarid)		1	500–200	18	T2	−21.8	−20.3	3.4	6.0	1.3	0.4
		6	500–200	34		−21.8 ± 0.4	−20.4 ± 0.4	6.3 ± 0.9	4.4 ± 1.3	n.d.	n.d.
Ostracoda		21	1000–500	15		−20.8	−19.2	6.8	6.2	2.7	1.7
		3	100–50	20	T2	−18.8 ± 0.4	−18.1 ± 0.5	8.0 ± 0.2	4.7 ± 0.2	n.d.	1.3 ± 0.0
Fish											
Cyclothone sp.		2	1000–200	4 + 15		−18.0/−19.8	−17.9/−19.3	12.4/10.3	4.1/4.5	3.8/3.7	3.5/2.7
		2	1000–500	31		−18.8/−18.5	−18.9/−18.4	10.0/11.4	3.9/4.1	n.d.	2.4/2.8

Trophic positions are calculated with lasis cylindrica [TP (I)] or POM [TP (P)] as reference levels. Asterisks mark samples collected from the southern study area recalculated for the North (stn. 4) accounting for the regional shift in $\delta^{15}N$ baseline. n (ind): number of samples (total number of individuals); C5: copepodid 5; f: females; m: males; juv: juveniles; n.d.: not determined, no baseline value available.

toward improving trophic position assessments via CSIA-AA (e.g., Ohkouchi et al., 2017; Ishikawa, 2018; Ramirez et al., 2021).

Selection of Food-Web Components as Reference for Baseline

In this study, we applied two different approaches to calculate trophic positions: Particulate organic matter (POM) as reference for TP 1 and a filter-feeding salp (*I. cylindrica*) as reference for TP 2.

Particulate organic matter generally consists of a very heterogeneous and largely unknown mixture of particles and organisms within the water column. It may vary significantly in isotope ratios (e.g., Stowasser et al., 2012; Pakhomov et al., 2019; Protopapa et al., 2019), as also observed in our study. As a result of its heterogeneity, POM does not only represent TP 1 (primary producers), but may include different trophic positions (Pakhomov et al., 2019), also shown in our data by the higher $\delta^{15}N$ values of POM compared to other organisms like salps or the copepod *N. minor*. Variation in $\delta^{15}N$ values also occurred between POM sampled at the surface vs. POM sampled at the chlorophyll maximum, highlighting the heterogeneous composition of POM.

Primary consumers, exhibiting lower turnover rates compared to phytoplankton, can provide a more stable baseline for isotopic studies (Cabana and Rasmussen, 1996). Several studies used filter-feeding salps as baseline for the calculation of trophic positions (e.g., Richoux and Froneman, 2009; Stowasser et al., 2012; Ménard et al., 2014). The use of salps for baseline values is also discussed controversially due to the involvement of these organisms in the microbial food web and knowledge gaps concerning food selection and contribution to the classical food web (Henschke et al., 2016; Pakhomov et al., 2019).

Copepods have also been used as baseline references in previous studies (e.g., Olson et al., 2010; Espinoza et al., 2017). However, copepods occupy a wide range of trophic positions, are often omnivorous and can shift their diets to adapt dynamically to local feeding conditions (e.g., Schukat et al., 2014; Henschke et al., 2015). In our study, the copepod with the lowest $\delta^{15}N$ was *N. minor* (<5‰ in the north, ∼9‰ in the south). This species is not described as a true herbivore. Also, samples of *N. minor* were only derived from a few stations. Therefore, we refrained from setting a TP (2 or 2.5) as baseline for this species. Instead, we chose POM and the salp *I. cylindrica* as reference baselines in the present study. *I. cylindrica* proved more realistic for TP determination, providing reasonable TPs for different species matching literature values. In contrast, the TP calculation with POM samples, with themselves rather high $\delta^{15}N$ ratios, delivered unrealistically low trophic positions (<2) for many mesozooplankton species (**Table 3**).

We applied an enrichment factor of 3.4‰ (e.g., Minagawa and Wada, 1984; Espinoza et al., 2017; Pizarro et al., 2019; Castro et al., 2020) to calculate trophic positions. Studies showed that

the enrichment factor is dependent on tissue and diet (Caut et al., 2009; Madigan et al., 2012; Bastos et al., 2017). Henschke et al. (2015) suggested a lower enrichment factor for zooplankton and Hussey et al. (2014) demonstrated that discrimination decreases with increasing $\delta^{15}N$ of the diet and therefore suggested decreasing discrimination factors with increasing trophic levels. Espinoza et al. (2017), however, reported no significant differences when applying fixed versus decreasing discrimination factors. Also modern approaches like the Bayesian estimation of trophic positions (Quezada-Romegialli et al., 2018) still use a default enrichment factor of 3.4‰.

Food-Web Structure and Key Players of the Northern Humboldt Current Upwelling System

Euphausiids are major contributors to macrozooplankton communities in eastern boundary upwelling systems (EBUS), while up to 90% of mesozooplankton abundance is comprised of copepods (e.g., Loick et al., 2005; Verheye et al., 2005; Antezana, 2010). In this study, we focus on medium to large-sized copepods [prosome length (PL) ca. 1–5 mm]. Nevertheless, small-sized copepods (PL $\leq$ 1 mm) can make a major contribution to biomass and secondary production, especially closer to the coast (Judkins, 1980; Criales-Hernández et al., 2008; Huggett et al., 2009) interlinking classical and microbial food webs (Calbet and Saiz, 2005; Vargas et al., 2007). However, in the northern HCS off Peru both juvenile and adult anchovies (*E. ringens*) forage mainly on euphausiids and larger-sized copepods (2–4 mm), i.e., *Eucalanus* and *Calanus* (e.g., Espinoza and Bertrand, 2008, 2014). In contrast to the Canary and Benguela Currents in the Atlantic, squat lobsters are important in the food webs of the California and Humboldt Currents in the Pacific (e.g., Gutiérrez et al., 2008; Espinoza et al., 2017). This is the first study presenting stable isotope as well as fatty acid profiles of various copepod species and other meso- and macrozooplankton components in the northern HCS off Peru. With regard to the major trophic pathways leading to the high fishery landings of anchovies, three dominant prey species of *E. ringens* (Espinoza and Bertrand, 2008) are key components in the pelagic food web of the northern HCS off Peru: the copepods *C. chilensis* and *E. inermis* (Judkins, 1980; Hirche et al., 2014; Schukat et al., 2021) and the krill *E. mucronata* (Riquelme-Bugueño et al., 2012; Kiko and Hauss, 2019). In addition, a fourth crustacean species, the squat lobster *P. monodon*, is an important component of the northern HCS food web (Gutiérrez et al., 2008; Espinoza et al., 2017).

Calanoid Copepods With Focus on *Calanus chilensis*: Concentrated Secondary Production and Food for Predators at Higher Trophic Positions in the Surface Layer

Most of the calanoid copepods in the surface layer occupied TPs of 2–2.5, referring to herbivorous and omnivorous feeding during the time of sampling. Smaller-sized copepods such as *Acartia tonsa* and *C. brachiatus* (PL ca. 1–1.5 mm) are very abundant in the northern HCS off Peru (e.g., Ayón et al., 2008a; Criales-Hernández et al., 2008). The genus *Centropages* feeds on a variety of prey items from phytoplankton to fish larvae with preferences for microheterotrophs (e.g., Turner et al., 1985; Calbet et al., 2007). This omnivorous feeding, including large amounts of ciliates and heterotrophic flagellates, may play an important role, interlinking the microbial loop and the 'classical food' chain (Calbet and Saiz, 2005; Calbet et al., 2007). Concerning the trophic pathways toward the anchovy, smaller-sized copepods, however, play a minor role as prey, whereas the larger-sized *Calanus* species are important prey items for anchovies (e.g., Espinoza and Bertrand, 2008, 2014). *C. chilensis* is endemic to the HCS, prevailing along the Chilean and Peruvian coast from ~3.5 to 45°S (e.g., Escribano et al., 2003; Hirche et al., 2014; Schukat et al., 2021). Although it is assumed to be herbivorous (Boyd et al., 1980), information about its feeding preferences is scarce. The low carnivory index of <0.3 together with the elevated amounts of diatom fatty acid markers with up to ~9% TFA in the present study point to a predominantly herbivorous feeding by *C. chilensis*. Calculated TPs of 1.9–2.2 for female *C. chilensis* using the salp *I. cylindrica* as baseline (TP = 2) support a herbivorous feeding habit of this copepod. *C. chilensis* is often restricted to the upper 50 m above the OMZ, reaching maximum abundances of 44,000 ind. m^{-2} (Escribano et al., 2009; Hirche et al., 2014; Schukat et al., 2021). Concentrated biomass of about 3 mg DM m^{-2} with secondary production extending from the coast far offshore in the northern HCS facilitates easy and efficient foraging on *C. chilensis* by planktivorous predators such as Peruvian anchovies (Schukat et al., 2021). Hence, *C. chilensis* represents a classical link between primary production and fish, thereby supporting a short and efficient food chain and high anchovy landings.

Euphausia mucronata: Dominant Krill Species With Diel Vertical Migration, Main Food Supply for Adult Anchovies

From personal observations during the research cruise MSM 80 and from published sources (e.g., Antezana, 2009, 2010), it is clear that *E. mucronata* is the dominant krill species in the northern HCS. This species alone occurs in densities of up to 16,500 ind. 1000 m^{-3}, whereas the following five most abundant euphausiid species together account for ≤1,600 individuals per 1,000 m^{-3} (Antezana, 2009), i.e., they are one order of magnitude less abundant. *E. mucronata* conducts extended diel vertical migrations from its daytime habitat at ca. 250 m in the OMZ to feed in the surface layer at night (Antezana, 2009). The species is well adapted to temporarily staying within the essentially anoxic OMZ. It shows a high activity of the enzyme lactate dehydrogenase providing sufficient energy without immediate oxygen demand in the OMZ during daytime (González and Quiñones, 2002; Tremblay and Abele, 2016). *E. mucronata* plays a major role in the carbon flux of the HCS due to its active transport of carbon through vertical migration and the passive transport via the production of large, fast-sinking fecal pellets (e.g., González et al., 2000, 2009). Furthermore, this species occupies a key role in the energy transfer of the HCS food web (e.g., Antezana, 2010). *E. mucronata* has the ability to shift to a more omnivorous diet, if phytoplankton is depleted (Riquelme-Bugueño et al., 2020) and can even prey on anchovy eggs (Krautz et al., 2007).

Filter-feeders consume a wide size range of food particles, in case of krill, from bacteria to mesozooplankton. They leave little space and opportunities for other, more specialized consumers. Hence, pelagic communities dominated by filter-feeders tend to be less complex with a reduced number of abundant species, limited major trophic pathways and, thus, a higher overall TTE. This has first been shown for lake ecosystems with water fleas (*Daphnia* spp.) as dominant filter-feeding zooplankton, but it also holds true for marine food webs, where often krill, thaliaceans and appendicularians are the important filter-feeders (Martin et al., 2017).

Our study highlights the different dietary preferences among euphausiid species in the northern HCS. *E. mucronata* had the lowest carnivory index compared to the other euphausiids. Its trophic position of ∼2.5 (via salp as TP 2) indicates herbivorous to omnivorous feeding. *E. mucronata* and *E. eximia* (TP: 2.1–2.9, CI: 0.4–0.5) are more herbivorous than *N. flexipes* and *Nematoscelis* sp. with TPs ∼3.0 and carnivory indices CIs of 0.7. *E. mucronata* is the mainstay in the diet of adult Peruvian anchoveta, providing >80% of the dietary carbon input (Espinoza and Bertrand, 2008, 2014; Espinoza et al., 2009). This species occupied TPs that were ∼1–1.5 lower than that of adult anchovy with TP 3.4 and the Pacific bonito with TP ∼4, supporting its role as prey source for pelagic fish. With its enormous biomass, *E. mucronata* indeed plays a key role in the rapid transfer of energy from primary producers to pelagic fish and other higher-level predators (Antezana, 2010). This represents a major trophic pathway, partially explaining the high trophic transfer efficiency of the HCS food web.

Pleuroncodes monodon: Benthic-Pelagic Coupling as "Inverse Export", a Unique Transfer of Organic Matter From the Seafloor to the Surface Layer?

Semi-pelagic squat lobsters are endemic and, therefore, unique to the Eastern Pacific EBUS, i.e., the California Current with *Pleuroncodes planipes* and the HCS with *P. monodon*. There are no ecological counterparts in the Canary and Benguela Currents. Early life stages of *P. monodon* are pelagic while juveniles and adults off Chile are bentho-demersal (e.g., Gallardo et al., 1993; Palma, 1994). In contrast, *P. monodon* off Peru was considered as fully pelagic (Gutiérrez et al., 2008). Elliott et al. (2011a,b) and Kiko et al. (2015), however, report a benthic occurrence of *P. monodon* also off Peru. These specimens remaining on the seafloor during daytime are well adapted to severely hypoxic or even anoxic conditions in shelf regions (Kiko et al., 2015). At least parts of the population conduct diel vertical migration, ascending to the surface layer at night, presumably to feed on phyto- and zooplankton and to replenish their oxygen debt. During research cruise MSM 80, we also found massive swarms of juvenile/adult *P. monodon* at the sea surface far away from the shelf over >5,000 m water depth. Therefore, a fully pelagic lifestyle (e.g., Gutiérrez et al., 2008) seems to be possible, at least temporarily. Most likely, squat lobsters feed rather opportunistically on benthic invertebrates and sulfur bacteria mats on the seafloor as well as on phyto- and zooplankton in the surface layer (Gallardo et al., 1994; Contreras et al., 2007; Funes et al., 2018).

In the present study, adult *P. monodon* from surface waters (50–0 m) had the highest δ^{13}C' values (North: −15.2 ± 0.6‰; Central: −14.7 ± 0.7‰) of all analyzed taxa. These values are similar to published δ^{13}C ratios of −16.0 to −14.3‰ (Espinoza et al., 2017). High δ^{13}C values are generally related to high productivity (Oczkowski et al., 2016) and may indicate that the foraging area of *P. monodon* is located within a smaller highly productive coastal zone (Espinoza et al., 2017). Samples of adult *P. monodon* for stable isotope analysis indeed derived from shelf stations (<150 m water depths). However, the difference in δ^{13}C' signals between POM and squat lobsters, from the same stations and water depths, was rather high with ∼4‰. Castro et al. (2020) determined on average ∼5‰ lower δ^{13}C ratios for POM as for macroalgae off Chile. The high *P. monodon* δ^{13}C' ratios of this study were in the range of those for Chlorophyta (−16.0 to −14.5‰) off central Chile (Castro et al., 2020). Potentially, high δ^{13}C' values could be due to ingestion of suspended particles (debris) of degraded macroalgae that drift away from the coastal zone (Miller and Page, 2012). Another explanation for the high δ^{13}C' ratios could be that *P. monodon* derive their food at least partly from benthic resources, similar to the squat lobster *Munida gregaria* (Funes et al., 2018). In this case, *P. monodon* could be a key player in benthic-pelagic coupling, comparable to the squat lobster *M. gregaria* found *inter alia* off Chile (Funes et al., 2018). Gallardo et al. (1994) suggested that mats of sulfur bacteria may serve as refuge and food source for *P. monodon* offspring. Polychaetes could be another potential benthic food source, for example *Paraprionospio pinnata* is known to dominate the benthic macrofauna off central Chile during non-El Niño years (Contreras et al., 2007). Feeding on sulfur bacteria and/or polychaetes would explain the high δ^{13}C' ratios of squat lobsters. If so, benthic feeding and diel vertical migration in *P. monodon* could provide a unique pathway for recovery of organic matter from the seafloor back to the surface layer, where squat lobsters are an important prey for larger pelagic fishes, such as bonitos, mackerels, and tunas (e.g., Bernard et al., 1985; Elliott and Paredes, 1996), and potentially sea lions and seabirds (Arias-Schereiber, 1996; Jahncke et al., 1998). The Pacific bonito as well as chub and jack mackerels are prominent species in the Peruvian fisheries (Produce–Peru, 2019). In the case of benthic feeding, our fourth hypothesis can be accepted, as the re-import of organic matter into the euphotic zone may also contribute to the exceptionally high trophic transfer efficiency of the HCS.

In earlier studies, Peruvian anchovies had δ^{13}C values similar to those of *P. monodon*, indicating an overlap in food source and foraging habitat. Similar δ^{15}N signals of the two species even suggested equivalent trophic positions with possible competition (Gutiérrez et al., 2008; Espinoza et al., 2017). Due to the opportunistic sampling of fish, anchovy samples covering the entire sampling area were not available for our analyses. These limited data do not show such an overlap in δ^{13}C' values of adult squat lobsters (−15.2 to −14.7‰) and anchovies (−16.6‰). Only the zoea larvae of *P. monodon* had wider δ^{13}C' ranges of −19.4 to −16.5‰ overlapping with the range of anchovies. Lower δ^{13}C' ratios in zoea larvae than in adult squat lobsters can be explained by the larvae feeding predominantly on pelagic primary production. δ^{15}N ratios of anchovies were ca. 3‰ higher

than those of adult *P. monodon*, indicating differences in trophic positions and feeding preferences.

Deviations between our data and published studies may be explained by the pronounced variability of $\delta^{15}N$ values (13.8–22.8‰) in anchovies, due to varying feeding preferences (Pizarro et al., 2019), different sampling seasons and locations or the use of different tissues with different turnover rates for the stable isotope analysis (Macneil et al., 2005; Jardine et al., 2006; Caut et al., 2009). Espinoza et al. (2017) analyzed anterior dorsal muscle tissue, whereas we used samples from caudal fins for the analyses.

Eucalanus Inermis and the Oxygen Minimum Zone

The important role of the extremely pronounced OMZ with an anoxic core between ca. 100 or 200 and 500 m depth in structuring the pelagic realm of the northern HCS has been highlighted in many studies (Hidalgo et al., 2005; Escribano et al., 2009; Hirche et al., 2014). *E. inermis*, the prevailing species among a complex of ∼five species of the genus *Eucalanus* in the HCS (Thiel et al., 2007), is the dominant calanoid copepod in the OMZ of the HCS (Flint et al., 1991; Hidalgo et al., 2005), well adapted to the OMZ with its low oxygen requirements (Hidalgo et al., 2005). Although this species may remain in the upper boundary of the OMZ with limited excursions into surface waters (Hidalgo et al., 2005), *Eucalanus* has been determined as an important copepod prey item of Peruvian anchovies (Espinoza and Bertrand, 2008).

In the present study, *E. inermis* had very variable mean $\delta^{15}N$ values of 9.5 to 15.2‰ mostly depending on their depth of occurrence. Individuals from the surface layer had a mean $\delta^{15}N$ ratio of ∼10‰ occupying a TP of 2, whereas individuals from the OMZ had higher and more variable mean $\delta^{15}N$ values of ∼10–15‰ (**Table 3**) occupying higher TPs from 3 to 5. The most likely explanation for this difference between surface- and OMZ-inhabiting individuals is that OMZ-inhabiting *E. inermis* feed at depth within the OMZ on older, degraded POM consisting of detritus and marine snow (Boyd et al., 1980; Altabet, 1988; Gaye-Haake et al., 2005). Surface-water POM mainly consists of fresh phytoplankton with low $\delta^{15}N$ ratios, whereas POM in the OMZ contains more degraded organic matter and detritus with higher $\delta^{15}N$ values. It is known from many ocean regions that the stable isotope ratios of POM increase with increasing water depth (e.g., Laakmann and Auel, 2010), as sinking organic particles are eaten and again egested as well as modified and restructured by zooplankton and microorganisms on their way to deeper layers. These processes result in further fractionations and enrichment of heavier isotopes. Thus, there is a baseline shift with regard to the $\delta^{15}N$ signal of POM with increasing water depth. Surface-dwelling *E. inermis* mainly feed on fresh phytoplankton with lower $\delta^{15}N$ values (present study; Williams, 2013). This is supported by carnivory indices of *E. inermis* suggesting a herbivorous to omnivorous feeding behavior (present study; Hidalgo et al., 2005; López-Ibarra et al., 2018).

The increase in $\delta^{15}N$ ratios of POM with increasing water depth also explains the well-known fact that deep-sea copepods, which exclusively consume sinking organic particles, usually have much higher $\delta^{15}N$ signals than suspension-feeding, i.e., mainly herbivorous, copepods in the surface layer. This has been clearly shown for copepod communities in the Benguela Current upwelling system (Schukat et al., 2014) and again in the present study for the HCS. Deep-sea copepods of the genera *Lucicutia*, *Gaetanus*, *Valdiviella*, *Bathycalanus*, *Metridia,* and predatory *Paraeuchaeta* from the OMZ had rather high $\delta^{15}N$ values between 10 and 16‰ (**Figure 5**). In contrast, all surface-dwelling copepods from the same northern investigation area had low $\delta^{15}N$ ratios <7‰, supporting our second hypothesis that the vertical differences in $\delta^{15}N$ ratios lead to higher $\delta^{15}N$ signals of suspension-feeding zooplankton permanently residing at depth compared to those of surface-living species or diel vertical migrants feeding at night in the surface layer.

In the same context, the rather low $\delta^{15}N$ ratios <10‰ of the decapod shrimps *Acanthephyra* and *Gennadas* as well as the peracarid *Gnathophausia* from the OMZ are rather surprising (**Figure 5**). Decapods are usually considered as carnivores. However, in the present study, the three species had lower $\delta^{15}N$ signals than almost all copepods from the same region and depth range. This observation raises the question of the major food sources of deep-sea decapods and *Gnathophausia* in the HCS. The most likely explanation would be that these species conduct diel vertical migrations and feed on POM and maybe copepods in the surface layer at night. Thus, they would incorporate the lower $\delta^{15}N$ signals of surface POM and zooplankton prey and carry it into their daytime habitat within the OMZ. The lower $\delta^{15}N$ signal of 7-8‰ of *Acanthephyra* would fit nicely to values of 4–5‰ for surface POM as potential prey, while higher values of 8–10‰ in *Gennadas* and *Gnathophausia* indicate a more omnivorous to carnivorous feeding behavior. Potentially, this may include surface-dwelling copepods with $\delta^{15}N$ signals of 4–6‰ in the northern part of the study area (**Figure 5**).

Toward Solving the "Peruvian Puzzle": Potential Reasons for the High Trophic Transfer Efficiency of the Humboldt Current Upwelling System

A highlight of the present study is its comprehensive assessment of trophic biomarkers in many species of the pelagic HCS community over a vast regional (8.5–16°S) and vertical range (regularly down to 1,000 m depth). Food webs associated with upwelling ecosystems are much more complex and dynamic than previously thought with diverse trophic interactions (Vargas et al., 2007; Espinoza and Bertrand, 2008; Schukat et al., 2014, 2021). With regard to the major trophic pathways leading toward the high anchovy landings our results indicate that five species seem to play a crucial role in the high TTE of the northern HCS: (i) the surface-dwelling copepod *C. chilensis*; two species with diel vertical migration: (ii) the krill *E. mucronata* and (iii) the squat lobster *P. monodon*, (iv) *E. inermis* as frequent inhabitant of the OMZ, and (v) the Peruvian anchovy *E. ringens*, the world's most important commercial fish species in terms of landings. These five species are key in the energy flux of the northern HCS, which leads to a rather limited number of major trophic pathways from primary producers to the Peruvian anchovy.

Moreover, the key species are characterized by specific and unusual life-cycle adaptations and characteristics that differ from

those of similar species in other EBUS and therefore most likely contribute to the enormous TTE of the northern HCS. *C. chilensis* deviates from the most relevant calanid copepods in other EBUS and higher latitudes by its lack of ontogenetic vertical migration, its lack of extensive lipid reserves and its lack of a dormant phase at depth (Schukat et al., 2021). Its biomass mostly remains compacted in the surface layer limited by the OMZ and provides a highly concentrated food supply and superb feeding conditions for Peruvian anchovies and sardines (*Sardinops sagax*).

In contrast to other EBUS, the secondary production of *C. chilensis* in the northern HCS extends much further offshore, up to 200 km from the coast (Schukat et al., 2021), resulting in a much larger area of high productivity. Similar suggestions were made by Espinoza et al. (2009) for the role of euphausiids. A higher availability of euphausiids attributed to the narrower shelf in the northern HCS compared to the Canary and Benguela systems might increase the importance of krill in the Pacific versus the Atlantic upwelling systems. During strong upwelling in the northern HCS, colder coastal waters can spread far from the shelf allowing coastal communities including small pelagic fish to extend their range of distribution far from the coast (Swartzman et al., 2008).

A unique feature of the HCS is the shallow and pronounced OMZ. The Peruvian anchovy is apparently not affected by a very shallow oxycline below 10 m (Bertrand et al., 2008, 2010) and benefits from the concentrated zooplankton biomass at the surface. Such concentrated prey may increase the fish carrying capacity (Bertrand et al., 2011). In contrast, in the other EBUS with a less pronounced and deeper OMZ, zooplankton exhibits a more extensive vertical distribution. Moreover, compared to other EBUS, the HCS probably has a higher zooplankton production related to a more efficient use of primary production by zooplankton and a strong connection between coastal and offshore pelagic ecosystems (Espinoza and Bertrand, 2008).

The semi-pelagic squat lobster *P. monodon* is not an important prey item of anchovies, but for many other pelagic fishes and apex predators, it represents a key component in the northern HCS food web. Benthic feeding on sulfur bacteria mats (Van Dover and Fry, 1989) and diel vertical migration of *P. monodon* would provide a unique energy transfer from the seafloor back to the surface layer. Such a "reverse" transport of organic matter could potentially reduce net export and increase the organic matter available for consumption in the surface layer. That would be a novel mechanism increasing the overall TTE in the HCS. In combination, all these factors support a structured food chain toward anchovies with an unusually high TTE in the HCS.

DATA AVAILABILITY STATEMENT

The original contributions presented in the study are included in the article/**Supplementary Material**, further inquiries can be directed to the corresponding author.

AUTHOR CONTRIBUTIONS

JM carried out the analyses and wrote the manuscript with support from AS, HA, DA, LK, EP, JC, and WH. AS, HA, WH, and JM contributed to the conceptual design and implementation of the research. All authors contributed to the article and approved the submitted version.

FUNDING

This study was part of the CUSCO project (Coastal Upwelling System in a Changing Ocean) funded by the German Federal Ministry of Education and Research (BMBF, 03F0813C). Funding for open access publication was provided by the University of Bremen.

ACKNOWLEDGMENTS

We thank the captain and crew of RV *Maria S. Merian* for their skillful support during the cruise MSM 80. Hydrobiological samples were collected in the Peruvian EEZ in cooperation with the Instituto del Mar del Perú (IMARPE) and according to the Resolución Directoral N°133-2018-MTC/13 issued on 20th December 2018 by the Dirección General de Transporte Acuatico. Special thanks go to Sabrina Dorschner for her help during fatty acid and stable isotope analysis. We are grateful to the Marine Biogeochemistry group at GEOMAR, Rainer Kiko and the Physical Oceanography team of Volker Mohrholz from the IOW for their support and for sharing their data. We also thank Martin Graeve and Niko Lahajnar for their support and fruitful discussions.

SUPPLEMENTARY MATERIAL

The Supplementary Material for this article can be found online at: https://www.frontiersin.org/articles/10.3389/fmars.2021.759603/full#supplementary-material

REFERENCES

Altabet, M. A. (1988). Variations in nitrogen isotopic composition between sinking and suspended particles: implications for nitrogen cycling and particle transformation in the open ocean. *Deep-Sea Res.* 35, 535–554. doi: 10.1016/0198-0149(88)90130-6

Antezana, T. (2009). Species-specific patterns of diel migration into the oxygen minimum zone by euphausiids in the Humboldt Current Ecosystem. *Prog. Oceanogr.* 83, 228–236. doi: 10.1016/j.pocean.2009.07.039

Antezana, T. (2010). *Euphausia mucronata*: A keystone herbivore and prey of the Humboldt Current System. *Deep-Sea Res. II* 57, 652–662. doi: 10.1016/j.dsr2.2009.10.014

Arias-Schereiber, M. (1996). Informe sobre el estado de conocimientos y conservación de los mamíferos marinos en el Perú. *Inf. Provisional Inst. Mar. Perú* 38:30.

Ayón, P., Criales-Hernández, M. I., Schwamborn, R., and Hirche, H.-J. (2008a). Zooplankton research off Peru: A review. *Prog. Oceanogr.* 79, 238–255. doi: 10.1016/j.pocean.2008.10.020

Ayón, P., Swartzman, G., Bertrand, A., Gutiérrez, M., and Bertrand, S. (2008b). Zooplankton and forage fish species off Peru: Large-scale bottom-up forcing and local-scale depletion. *Prog. Oceanogr.* 79, 208–214. doi: 10.1016/j.pocean.2008.10.023

Bakun, A., and Weeks, S. J. (2008). The marine ecosystem off Peru: What are the secrets of its fishery productivity and what might its future hold? *Prog. Oceanogr.* 79, 290–299. doi: 10.1016/j.pocean.2008.10.027

Bastos, R. F., Corrêa, F., Winemiller, K. O., and Garcia, A. M. (2017). Are you what you eat? Effects of trophic discrimination factors on estimates of food assimilation and trophic position with a new estimation method. *Ecol. Indic.* 75, 234–241. doi: 10.1016/j.ecolind.2016.12.007

Bernard, H. J., Hedgepeth, J. B., and Reilly, S. B. (1985). Stomach contents of albacore, skipjack, and bonito caught off southern California during summer 1983. *CalCOFI Rep.* 26, 175–182.

Bertrand, A., Ballón, M., and Chaigneau, A. (2010). Acoustic observation of living organisms reveals the upper limit of the oxygen minimum zone. *PLoS One* 5:e10330. doi: 10.1371/journal.pone.0010330e1

Bertrand, A., Chaigneau, A., Peraltilla, S., Ledesma, J., Graco, M., Monetti, F., et al. (2011). Oxygen: A fundamental property regulating pelagic ecosystem structure in the coastal southeastern tropical Pacific. *PLoS One* 6:e29558. doi: 10.1371/journal.pone.0029558

Bertrand, A., Gerlotto, F., Bertrand, S., Guitiérrez, M., Alza, L., Chipollini, A., et al. (2008). Schooling behaviour and environmental forcing in relation to anchoveta distribution: An analysis across multiple spatial scales. *Prog. Oceanogr.* 79, 264–277. doi: 10.1016/j.pocean.2008.10.018

Bertrand, A., Segura, M., Gutiérrez, M., and Vásquez, L. (2004). From small-scale habitat loopholes to decadal cycles: a habitat-based hypothesis explaining fluctuation in pelagic fish populations off Peru. *Fish Fish.* 5, 296–316. doi: 10.1111/j.1467-2679.2004.00165.x

Bicknell, A. W., Campbell, M., Knight, M. E., Bilton, D. T., Newton, J., and Votier, S. C. (2011). Effects of formalin preservation on stable carbon and nitrogen isotope signatures in Calanoid copepods: implications for the use of Continuous Plankton Recorder Survey samples in stable isotope analyses. *Rapid Commun. Mass Spectrom.* 25, 1794–1800. doi: 10.1002/rcm.5049

Bode, M., Hagen, W., Schukat, A., Teuber, L., Fonseca-Batista, D., Dehairs, F., et al. (2015). Feeding strategies of tropical and subtropical calanoid copepods throughout the eastern Atlantic Ocean - Latitudinal and bathymetric aspects. *Prog. Oceanogr.* 138, 268–282. doi: 10.1016/j.pocean.2015.10.002

Boyd, C. M., Smith, S. L., and Cowles, T. J. (1980). Grazing patterns of copepods in the upwelling system off Peru. *Limnol. Oceanogr.* 25, 583–596. doi: 10.4319/lo.1980.25.4.0583

Cabana, G., and Rasmussen, J. B. (1996). Comparison of aquatic food chains using nitrogen isotopes. *Proc. Natl. Acad. Sci. U. S. A.* 93, 10844–10847. doi: 10.1073/pnas.93.20.10844

Calbet, A., and Saiz, E. (2005). The ciliate-copepod link in marine ecosystems. *Aquat. Microb. Ecol.* 38, 157–167.

Calbet, A., Carlotti, F., and Gaudy, R. (2007). The feeding ecology of the copepod *Centropages typicus* (Kröyer). *Prog. Oceanogr.* 72, 137–150.

Castillo, R., Dalla Rosa, L., García Diaz, W., Madureira, L., Gutierrez, M., Vásquez, L., et al. (2019). Anchovy distribution off Peru in relation to abiotic parameters: A 32-year time series from 1985 to 2017. *Fish. Oceanogr.* 28, 389–401. doi: 10.1111/fog.12419

Carr, M.-E. (2002). Estimation of potential productivity in Eastern Boundary Currents using remote sensing. *Deep Sea Res. II Top. Stud. Oceanogr.* 49, 59–80. doi: 10.1016/S0967-0645(01)00094-7

Castro, L. R., González, V., Claramunt, G., Barrientos, P., and Soto, S. (2020). Stable isotopes ($\delta^{13}C$, $\delta^{15}N$) seasonal changes in particulate organic matter and in different life stages of anchoveta (*Engraulis ringens*) in response to local and large scale oceanographic variations in north and central Chile. *Prog. Oceanogr.* 186:102342. doi: 10.1016/j.pocean.2020.102342

Caut, S., Angulo, E., and Courchamp, F. (2009). Variation in discrimination factors ($\Delta^{15}N$ and $\Delta^{13}C$): the effect of diet isotopic values and applications for diet reconstruction. *J. Appl. Ecol.* 46, 443–453. doi: 10.1111/j.1365-2664.2009.01620.x

Chavez, F. P., and Messié, M. (2009). A comparison of Eastern Boundary Upwelling Ecosystems. *Prog. Oceanogr.* 83, 80–96. doi: 10.1016/j.pocean.2009.07.032

Contreras, S., Pantoja, S., Neira, C., and Lange, C. B. (2007). Biogeochemistry of surface sediments off Concepción (∼36°S), Chile: El Niño vs. non-El Niño conditions. *Prog. Oceanogr.* 75, 576–585. doi: 10.1016/j.pocean.2007.08.030

Chavez, F. P., Bertrand, A., Guevara-Carrasco, R., Soler, P., and Csirke, J. (2008). The northern Humboldt Current System: Brief history, present status and a view towards the future. *Prog. Oceanogr.* 79, 95–105. doi: 10.1016/j.pocean.2008.10.012

Chikaraishi, Y., Ogawa, N. O., Kashiyama, Y., Takano, Y., Suga, H., Tomitani, A., et al. (2009). Determination of aquatic food-web structure based on compound-specific nitrogen isotopic composition of amino acids. *Limnol. Oceanogr. Methods* 7, 740–750.

Criales-Hernández, M. I., Schwamborn, R., Graco, M., Ayón, P., Hirche, H.-J., and Wolff, M. (2008). Zooplankton vertical distribution and migration off Central Peru in relation to the oxygen minimum layer. *Helgol. Mar. Res.* 62(Suppl. 1), S85–S100. doi: 10.1007/s10152-007-0094-3

Dalsgaard, J., St. John, M., Kattner, G., Müller-Navarra, D., and Hagen, W. (2003). Fatty acid trophic markers in the pelagic marine environment. *Adv. Mar. Biol.* 46, 225–340. doi: 10.1016/s0065-2881(03)46005-7

Doering, K., Ehlert, C., Martinez, P., Frank, M., and Schneider, R. (2019). Latitudinal variations in $\delta^{30}Si$ and $\delta^{15}N$ signatures along the Peruvian shelf: quantifying the effects of nutrient utilization versus denitrification over the past 600 years. *Biogeosciences* 16, 2163–2180. doi: 10.5194/bg-16-2163-2019

Elliott, W., and Paredes, F. (1996). Estructura especiológica del subsistema costero, Prospección 9512-9601. *Inf. Inst. Mar. Perú* 121, 14–26.

Elliott, W., Caccha, L., and Benites, C. (2011a). Estructura del subsistema demersal en otoño 2003. Crucero BIC Olaya 0305-06. *Inf. Inst. Mar. Perú* 38, 197–202.

Elliott, W., Caccha, L., and Benites, C. (2011b). Estructura del subsistema demersal durante el verano 2004. Crucero BIC Olaya 0401-02. *Inf. Inst. Mar. Perú* 38, 321–334.

Escribano, R., Fernández, M., and Aranís, A. (2003). Physical-chemical processes and patterns of diversity of the Chilean eastern boundary pelagic and benthic marine ecosystems: an overview. *Gayana* 67, 190–205.

Escribano, R., Hidalgo, P., and Krautz, C. (2009). Zooplankton associated with the oxygen minimum zone system in the northern upwelling region of Chile during March 2000. *Deep-Sea Res. II* 56, 1083–1094. doi: 10.1016/j.dsr2.2008.09.009

Espinoza, P., and Bertrand, A. (2008). Revisiting Peruvian anchovy (*Engraulis ringens*) trophodynamics provides a new vision of the Humboldt Current system. *Prog. Oceanogr.* 79, 215–227. doi: 10.1016/j.pocean.2008.10.022

Espinoza, P., and Bertrand, A. (2014). Ontogenetic and spatiotemporal variability in anchoveta *Engraulis ringens* diet off Peru. *J. Fish Biol.* 84, 422–435. doi: 10.1111/jfb.12293

Espinoza, P., Bertrand, A., van der Lingen, C. D., Garrido, S., Rojas, and de Mendiola, B. (2009). Diet of sardine (*Sardinops sagax*) in the northern Humboldt Current system and comparison with the diets of clupeoids in this and other eastern boundary upwelling systems. *Prog. Oceanogr.* 83, 242–250. doi: 10.1016/j.pocean.2009.07.045

Espinoza, P., Lorrain, A., Ménard, F., Cherel, Y., Tremblay-Boyer, L., Argüelles, J., et al. (2017). Trophic structure in the northern Humboldt Current system: new perspectives from stable isotope analysis. *Mar. Biol.* 164, 1–15. doi: 10.1007/s00227-017-3119-8

Flint, M. V., Drits, A. V., and Pasternak, A. F. (1991). Characteristic features of body composition and metabolism in some interzonal copepods. *Mar. Biol.* 111, 199–205. doi: 10.1007/BF0131970

Folch, J., Lees, M., and Sloane Stanley, G. H. (1957). A simple method for the isolation and purification of total lipids from animal tissues. *J. Biol. Chem.* 226, 479–509. doi: 10.1007/s10858-011-9570-9

France, R. L., and Peters, R. H. (1997). Ecosystem differences in the trophic enrichment of ^{13}C in aquatic food webs. *Can. J. Fish. Aquat. Sci.* 54, 1255–1258. doi: 10.1139/f97-044

Fuenzalida, R., Schneider, W., Garcés-Vargas, J., Bravo, L., and Lange, C. (2009). Vertical and horizontal extension of the oxygen minimum zone in the eastern South Pacific Ocean. *Deep-Sea Res. II* 56, 1027–1038. doi: 10.1016/j.dsr2.2008.11.001

Funes, M., Irigoyen, A. J., Trobbiani, G. A., and Galván, D. E. (2018). Stable isotopes reveal different dependencies on benthic and pelagic pathways between *Munida gregaria* ecotypes. *Food Webs* 16, 1–9. doi: 10.1016/j.fooweb.2018.e00101

Gallardo, V. A., Cañete, J. I., Enríquez-Briones, S., Roa, R., Acuña, A., and Baltazar, M. (1993). "Biología del langostino colorado *Pleuroncodes monodon* H. Milne Edwards, 1837 y especies afines (Crustacea, Decapoda, Anomura, Galatheidae): sinopsis," in *Elementos Básicos Para la Gestión de Los Recursos Vivos Marinos Costeros de la Región del Biobío*, Vol. 2, eds F. Faranda and O. Parra (Concepción: Monografías Científicas EULA-Chile), 67–113.

Gallardo, V. A., Cañete, J. I., Roa, R., Enríquez-Briones, S., and Baltazar, M. (1994). Recruitment of the squat lobster *Pleuroncodes monodon* on the continental shelf off central Chile. *J. Crustac. Biol.* 14, 665–669. doi: 10.1163/193724094X00632

Gaye-Haake, B., Lahajnar, N., Emeis, K. C., Unger, D., Rixen, T., Suthhof, A., et al. (2005). Stable nitrogen isotopic ratios of sinking particles and sediments from the northern Indian Ocean. *Mar. Chem.* 96, 243–255. doi: 10.1016/j.marchem.2005.02.001

González, H. E., Daneri, G., Iriarte, J. L., Yannicelli, B., Menschel, E., Barría, C., et al. (2009). Carbon fluxes within the epipelagic zone of the Humboldt Current System off Chile: The significance of euphausiids and diatoms as key functional groups for the biological pump. *Prog. Oceanogr.* 83, 217–227. doi: 10.1016/j.pocean.2009.07.036

González, H. E., Ortiz, V. C., and Sobarzo, M. (2000). The role of faecal material in the particulate organic carbon flux in the northern Humboldt Current, Chile (23°S), before and during the 1997–1998 El Niño. *J. Plankton Res.* 22, 499–529.

González, R. R., and Quiñones, R. A. (2002). Ldh activity in *Euphausia mucronata* and *Calanus chilensis*: Implications for vertical migration behaviour. *J. Plankton Res.* 24, 1349–1356. doi: 10.1093/plankt/24.12.1349

Graeve, M., Hagen, W., and Kattner, G. (1994). Herbivorous or omnivorous? On the significance of lipid compositions as trophic markers in Antarctic copepods. *Deep-Sea Res. I* 41, 915–924. doi: 10.1016/0967-0637(94)90083-3

Graham, B. S., Koch, P. L., Newsome, S. D., McMahon, K. W., and Aurioles, D. (2010). "Using isoscapes to trace the movements and foraging behavior of top predators in oceanic ecosystems," in *Isoscapes: Understanding Movement, Pattern, and Process on Earth Through Isotope Mapping*, eds J. B. West, G. J. Bowen, T. E. Dawson, and K. P. Tu (Berlin: Springer), 299–318. doi: 10.1007/978-90-481-3354-3

Granger, J., Sigman, D. M., Needoba, J. A., and Harrison, P. J. (2009). Coupled nitrogen and oxygen isotope fractionation of nitrate during assimilation by cultures of marine phytoplankton. *Limnol. Oceanogr.* 49, 1763–1773. doi: 10.4319/lo.2004.49.5.1763

Gutiérrez, M., Ramirez, A., Bertrand, S., Móron, O., and Bertrand, A. (2008). Ecological niches and areas of overlap of the squat lobster "munida" (*Pleuroncodes monodon*) and anchoveta (*Engraulis ringens*) off Peru. *Prog. Oceanogr.* 79, 256–263. doi: 10.1016/j.pocean.2008.10.019

Hagen, W., Postel, L., and Fock, H. (2000). "Biomass and abundance," in *ICES Zooplankton Methodology Manual*, eds R. Harris, et al. (San Diego: Academy Press), 83–192. doi: 10.1016/B978-012327645-2/50005-0

Hannides, C. C. S., Popp, B. N., Landry, M. R., and Graham, B. S. (2009). Quantification of zooplankton trophic position in the North Pacific Subtropical Gyre using stable nitrogen isotopes. *Limnol. Oceanogr.* 54, 50–61. doi: 10.4319/lo.2009.54.1.0050

Henschke, N., Everett, J. D., Richardson, A. J., and Suthers, I. M. (2016). Rethinking the role of salps in the ocean. *Trends Ecol. Evol.* 31, 720–733. doi: 10.1016/j.tree.2016.06.007

Henschke, N., Everett, J. D., Suthers, I. M., Smith, J. A., Hunt, B. P. V., Doblin, M. A., et al. (2015). Zooplankton trophic niches respond to different water types of the western Tasman Sea: A stable isotope analysis. *Deep-Sea Res. I* 104, 1–8. doi: 10.1016/j.dsr.2015.06.010

Hetherington, E. D., Olson, R. J., Drazen, J. C., Lennert-Cody, C. E., Ballance, L. T., Kaufmann, R. S., et al. (2017). Spatial food-web structure in the eastern tropical Pacific Ocean based on compound-specific nitrogen isotope analysis of amino acids. *Limnol. Oceanogr.* 62, 541–560. doi: 10.1002/lno.10443

Hidalgo, P., Escribano, R., and Morales, C. E. (2005). Ontogenetic vertical distribution and diel migration of the copepod *Eucalanus inermis* in the oxygen minimum zone off northern Chile (20-21° S). *J. Plankton Res.* 27, 519–529. doi: 10.1093/plankt/fbi025

Hirche, H. J., Barz, K., Ayón, P., and Schulz, J. (2014). High resolution vertical distribution of the copepod *Calanus chilensis* in relation to the shallow oxygen minimum zone off northern Peru using LOKI, a new plankton imaging system. *Deep-Sea Res. I* 88, 63–73. doi: 10.1016/j.dsr.2014.03.001

Hobson, K. A., and Welch, H. E. (1992). Determination of trophic relationships within a high Arctic marine food web using $\delta^{13}C$ and $\delta^{15}N$ analysis. *Mar. Ecol. Prog. Ser.* 84, 9–18.

Hobson, K. A., Fisk, A., Karnovsky, N., Holst, M., Gragnon, J.-M., and Fortier, M. (2002). A stable isotope ($\delta^{13}C$, $\delta^{15}N$) model for the North Water food web: implications for evaluating trophodynamics and the flow of energy and contaminants. *Deep-Sea Res. II* 49, 5131–5150. doi: 10.1016/S0967-0645(02)00182-0

Huggett, J., Verheye, H., Escribano, R., and Fairweather, T. (2009). Copepod biomass, size composition and production in the Southern Benguela: Spatio–temporal patterns of variation, and comparison with other eastern boundary upwelling systems. *Prog. Oceanogr.* 83, 197–207.

Hussey, N. E., MacNeil, M. A., McMeans, B. C., Olin, J. A., Dudley, S. F. J., Cliff, G., et al. (2014). Rescaling the trophic structure of marine food webs. *Ecol. Lett.* 17, 239–250. doi: 10.1111/ele.12226

Ishikawa, N. F. (2018). Use of compound-specific nitrogen isotope analysis of amino acids in trophic ecology: assumptions, applications, and implications. *Ecol. Res.* 33, 825–837. doi: 10.1007/s11284-018-1616-y

Jahncke, J., Ayala, L., and Mendoza, C. (1998). Abundancia relativa y distribución de aves marinas frente a la costa peruana y su relación con la abundancia de anchoveta Crucero BIC Humboldt 9808-09 de Piura a Lima. *Inf. Inst. Mar Perú* 141, 85–95.

Jardine, T. D., Kidd, K. A., and Fisk, A. T. (2006). Applications, considerations, and sources of uncertainty when using stable isotope analysis in ecotoxicology. *Environ. Sci. Technol.* 40, 7501–7511. doi: 10.1021/es061263h

Jarre-Teichmann, A. (1998). The potential role of mass balance models for the management of upwelling ecosystems. *Ecol. Appl.* 8, 93–103.

Judkins, D. C. (1980). Vertical distribution of zooplankton in relation to the oxygen minimum off Peru. *Deep-Sea Res. I: Oceanogr. Res. Pap.* 27A, 475–487.

Kattner, G., Albers, C., Graeve, M., and Schnack-Schiel, S. B. (2003). Fatty acid and alcohol composition of the small polar copepods, *Oithona* and *Oncaea*: Indication on feeding modes. *Polar Biol.* 26, 666–671. doi: 10.1007/s00300-003-0540-x

Kattner, G., and Hagen, W. (1995). Polar herbivorous copepods - different pathways in lipid biosynthesis. *ICES J. Mar. Sci.* 52, 329–335. doi: 10.1016/1054-3139(95)80048-4

Kattner, G., Graeve, M., and Hagen, W. (1994). Ontogenetic and seasonal changes in lipid and fatty acid/alcohol compositions of the dominant Antarctic copepods *Calanus propinquus*, *Calanoides acutus* and *Rhincalanus gigas*. *Mar. Biol.* 644, 637–644. doi: 10.1007/BF00347511

Kiko, R., and Hauss, H. (2019). On the estimation of zooplankton-mediated active fluxes in oxygen minimum zone regions. *Front. Mar. Sci.* 6:741. doi: 10.3389/fmars.2019.00741

Kiko, R., Hauss, H., Dengler, M., Sommer, S., and Melzner, F. (2015). The squat lobster *Pleuroncodes monodon* tolerates anoxic "dead zone" conditions off Peru. *Mar. Biol.* 162, 1913–1921. doi: 10.1007/s00227-015-2709-6

Krautz, M. C., Castro, L. R., and González, M. (2007). Interaction of two key pelagic species in the Humboldt Current: euphausiid predation on anchoveta eggs estimated by immunoassays. *Mar. Ecol. Prog. Ser.* 335, 175–185.

Laakmann, S., and Auel, H. (2010). Longitudinal and vertical trends in stable isotope signatures ($\delta^{13}C$ and $\delta^{15}N$) of omnivorous and carnivorous copepods across the South Atlantic Ocean. *Mar. Biol.* 157, 463–471. doi: 10.1007/s00227-009-1332-9

Larsen, T., Ventura, M., Andersen, N., O'Brien, D. M., Piatkowski, U., and McCarthy, M. D. (2013). Tracing carbon sources through aquatic and terrestrial food webs using amino acid stable isotope fingerprinting. *PLoS One* 8:1–9. doi: 10.1371/journal.pone.0073441

Loick, N., Ekau, W., and Verheye, H. M. (2005). Water-body preferences of dominant calanoid copepod species in the Angola-Benguela frontal zone. *African J. Mar. Sci.* 27, 597–608. doi: 10.2989/18142320509504120

López-Ibarra, G. A., Bode, A., Hernández-Trujillo, S., Zetina-Rejón, M. J., and Arreguín-Sánchez, F. (2018). Trophic position of twelve dominant pelagic copepods in the eastern tropical Pacific Ocean. *J. Mar. Syst.* 187, 13–22. doi: 10.1016/j.jmarsys.2018.06.009

Macneil, M. A., Skomal, G. B., and Fisk, A. T. (2005). Stable isotopes from multiple tissues reveal diet switching in sharks. *Mar. Ecol. Prog.* 302, 199–206. doi: 10.3354/meps302199

Madigan, D. J., Litvin, S. Y., Popp, B. N., Carlisle, A. B., Farwell, C. J., and Block, B. A. (2012). Tissue turnover rates and isotopic trophic discrimination factors in the endothermic teleost, Pacific bluefin tuna (*Thunnus orientalis*). *PLoS One* 7:1–13. doi: 10.1371/journal.pone.0049220

Martin, B., Koppelmann, R., and Kassatov, P. (2017). Ecological relevance of salps and doliolids in the northern Benguela Upwelling System. *J. Plankton Res.* 39, 290–304. doi: 10.1093/plankt/fbw095

McClelland, J. W., and Montoya, J. P. (2002). Trophic relationships and the nitrogen isotopic composition of amino acids in plankton. *Ecology* 83, 2173–2180.

Ménard, F., Benivary, H. D., Bodin, N., Coffineau, N., Le Loc'h, F., Mison, T., et al. (2014). Stable isotope patterns in micronekton from the Mozambique Channel. *Deep-Sea Res. II* 100, 153–163. doi: 10.1016/j.dsr2.2013.10.023

Miller, R. J., and Page, H. M. (2012). Kelp as a trophic resource for marine suspension feeders: a review of isotope-based evidence. *Mar. Biol.* 159, 1391–1402.

Minagawa, M., and Wada, E. (1984). Stepwise enrichment of ^{15}N along food chains: Further evidence and the relation between δ^{15}N and animal age. *Geochim. Cosmochim. Acta* 48, 1135–1140. doi: 10.1016/0016-7037(84)90204-7

Mintenbeck, K., Brey, T., Jacob, U., Knust, R., and Struck, U. (2008). How to account for the lipid effect on carbon stable-isotope ratio (δ^{13}C): Sample treatment effects and model bias. *J. Fish Biol.* 72, 815–830. doi: 10.1111/j.1095-8649.2007.01754.x

Mollier-Vogel, E., Ryabenko, E., Martinez, P., Wallace, D., Altabet, M. A., and Schneider, R. (2012). Nitrogen isotope gradients off Peru and Ecuador related to upwelling, productivity, nutrient uptake and oxygen deficiency. *Deep-Sea Res. I* 70, 14–25. doi: 10.1016/j.dsr.2012.06.003

Oczkowski, A., Kreakie, B., McKinney, R. A., and Prezioso, J. (2016). Patterns in stable isotope values of nitrogen and carbon in particulate matter from the northwest Atlantic continental shelf, from the Gulf of Maine to Cape Hatteras. *Front. Mar. Sci.* 3:1–9. doi: 10.3389/fmars.2016.00252

Ohkouchi, N., Chikaraishi, Y., Close, H. G., Fry, B., Larsen, T., Madigan, D. J., et al. (2017). Advances in the application of amino acid nitrogen isotopic analysis in ecological and biogeochemical studies. *Org. Geochem.* 113, 150–174. doi: 10.1016/j.orggeochem.2017.07.009

Olson, R. J., Popp, B. N., Graham, B. S., López-Ibarra, G. A., Galván-Magaña, F., Lennert-Cody, C. E., et al. (2010). Food-web inferences of stable isotope spatial patterns in copepods and yellowfin tuna in the pelagic eastern Pacific Ocean. *Prog. Oceanogr.* 86, 124–138. doi: 10.1016/j.pocean.2010.04.026

Pakhomov, E. A., Henschke, N., Hunt, B. P. V., Stowasser, G., and Cherel, Y. (2019). Utility of salps as a baseline proxy for food web studies. *J. Plankton Res.* 41, 3–11. doi: 10.1093/plankt/fby051

Palma, S. (1994). Distribución y abundancia de larvas de langostino colorado Pleuroncodes monodon frente a la costa de Concepción, Chile. Invest. Mar. 22, 13–29. doi: 10.4067/s0717-71781994002200002

Peterson, B. J., and Fry, B. (1987). Stable isotopes in ecosystem studies. *Annu. Rev. Ecol. Syst.* 18, 293–320. doi: 10.1146/annurev.es.18.110187.001453

Pizarro, J., Docmac, F., and Harrod, C. (2019). Clarifying a trophic black box: stable isotope analysis reveals unexpected dietary variation in the Peruvian anchovy *Engraulis ringens*. *PeerJ* 7:e6968. doi: 10.7717/peerj.6968

Post, D. M. (2002). Using stable isotopes to estimate trophic positions: Models, methods and assumptions. *Ecology* 83, 703–718. doi: 10.2307/3071875

Produce–Peru. (2019). *Anuario Estadístico Pesquero y Acuícola 2018*. Lima: Ministerio de la Producción.

Protopapa, M., Koppelmann, R., Zervoudaki, S., Wunsch, C., Peters, J., Parinos, C., et al. (2019). Trophic positioning of prominent copepods in the epi- and mesopelagic zone of the ultra-oligotrophic eastern Mediterranean Sea. *Deep-Sea Res. II* 164, 144–155. doi: 10.1016/j.dsr2.2019.04.011

Quezada-Romegialli, C., Jackson, A. L., Hayden, B., Kahilainen, K. K., Lopes, C., and Harrod, C. (2018). tRophicPosition, an r package for the Bayesian estimation of trophic position from consumer stable isotope ratios. *Methods Ecol. Evol.* 9, 1592–1599. doi: 10.1111/2041-210X.13009

Ramirez, M. D., Besser, A. C., Newsome, S. D., and McMahon, K. W. (2021). Meta-analysis of primary producer amino acid δ15N values and their influence on trophic position estimation. *Methods Ecol. Evol.* 12, 1750–1767. doi: 10.1111/2041-210X.13678

Richoux, N. B., and Froneman, P. W. (2009). Plankton trophodynamics at the subtropical convergence, Southern Ocean. *J. Plankton Res.* 31, 1059–1073. doi: 10.1093/plankt/fbp054

Riquelme-Bugueño, R., Núñez, S., Jorquera, E., Valenzuela, L., Escribano, R., and Hormazábal, S. (2012). The influence of upwelling variation on the spatially-structured euphausiid community off central-southern Chile in 2007-2008. *Prog. Oceanogr.* 92–95, 146–165. doi: 10.1016/j.pocean.2011.07.003

Riquelme-Bugueño, R., Pantoja-Gutiérrez, S., Jorquera, E., Anabalón, V., Srain, B., and Schneider, W. (2020). Fatty acid composition in the endemic Humboldt Current krill, *Euphausia mucronata* (Crustacea, Euphausiacea) in relation to the phytoplankton community and oceanographic variability off Dichato coast in central Chile. *Prog. Oceanogr.* 188:102425. doi: 10.1016/j.pocean.2020.102425

Schukat, A., Auel, H., Teuber, L., Lahajnar, N., and Hagen, W. (2014). Complex trophic interactions of calanoid copepods in the Benguela upwelling system. *J. Sea Res.* 85, 186–196. doi: 10.1016/j.seares.2013.04.018

Schukat, A., Wilhelm, H., Dorschner, S., Correa Acosta, J., Pinedo Arteaga, E. L., Ayón, P., et al. (2021). Zooplankton ecology traits maximize the trophic transfer efficiency of the Humboldt Current upwelling system. *Prog. Oceanogr.* 193:102551. doi: 10.1016/j.pocean.2021.102551

Sigman, O. M., Altabet, M. A., McCorkle, D. C., Francois, R., and Fischer, G. (1999). The δ^{15}N of nitrate in the Southern Ocean: Consumption of nitrate in surface waters. *Global Biogeochem. Cycles* 13, 1149–1166. doi: 10.1029/1999GB900038

Smyntek, P. M., Teece, M. A., Schulz, K. L., and Thackeray, S. J. (2007). A standard protocol for stable isotope analysis of zooplankton in aquatic food web research using mass balance correction models. *Limnol. Oceanogr.* 52, 2135–2146. doi: 10.4319/lo.2007.52.5.2135

Stowasser, G., Atkinson, A., McGill, R. A. R., Phillips, R. A., Collins, M. A., and Pond, D. W. (2012). Food web dynamics in the Scotia Sea in summer: A stable isotope study. *Deep-Sea Res. II* 5, 208–221. doi: 10.1016/j.dsr2.2011.08.004

Swartzman, G., Bertrand, A., Gutiérrez, M., Bertrand, S., and Vasquez, L. (2008). The relationship of anchovy and sardine to water masses in the Peruvian Humboldt Current system from 1983 to 2005. *Prog. Oceanogr.* 79, 228–237. doi: 10.1016/j.pocean.2008.10.021

Thiel, M., Macaya, E. C., Acuña, E., Arntz, W. E., Bastias, H., Brokordt, K., et al. (2007). The Humboldt Current systems of northern and central Chile, oceanographic processes, ecological interactions and socioeconomic feedback. *Oceanogr. Mar. Biol.* 45, 195–344.

Tremblay, N., and Abele, D. (2016). Response of three krill species to hypoxia and warming: an experimental approach to oxygen minimum zones expansion in coastal ecosystems. *Mar. Ecol.* 37, 179–199. doi: 10.1111/maec.12258

Turner, J. T., Tester, P. A., and Hettler, W. F. (1985). Zooplankton feeding ecology: a laboratory study of predation on fish eggs and larvae by the copepods *Anomalocera ornata* and *Centropages typicus*. *Mar. Biol.* 90, 1–8.

Van Dover, C. L., and Fry, B. (1989). Stable isotopic compositions of hydrothermal vent organisms. *Mar. Biol.* 102, 257–263. doi: 10.1007/BF00428287

Vargas, C. A., Martínez, R. A., Cuevas, L. A., Pavez, M. A., Cartes, C., González, H. E., et al. (2007). The relative importance of microbial and classical food webs in a highly productive coastal upwelling area. *Limnol. Oceanogr.* 52, 1495–1510.

Verheye, H. M., Hagen, W., Auel, H., Ekau, W., Loick, N., Rheenen, I., et al. (2005). Life strategies, energetics and growth characteristics of *Calanoides carinatus* (Copepoda) in the Angola-Benguela frontal region. *African J. Mar. Sci.* 27, 641–651. doi: 10.2989/18142320509504124

Williams, R. (2013). *Trophic Ecology of Oxygen Minimum Zone Zooplankton Revealed by Carbon and Nitrogen Stable Isotopes*. Open Access Dissertations. Paper 130. Kingston, RI: University of Rhode Island, doi: 10.23860/diss-williams-rebecca-2013

Conflict of Interest: The authors declare that the research was conducted in the absence of any commercial or financial relationships that could be construed as a potential conflict of interest.

Publisher's Note: All claims expressed in this article are solely those of the authors and do not necessarily represent those of their affiliated organizations, or those of the publisher, the editors and the reviewers. Any product that may be evaluated in this article, or claim that may be made by its manufacturer, is not guaranteed or endorsed by the publisher.